# Neural signal recording and processing in somatic neuroprosthetic applications. A Review.

Stanisa Raspopovic [1], Andrea Cimolato [1,2,3,], Alessandro Panarese [4], Fabio Vallone [4], Jaume del Valle [5], Silvestro Micera [4,6], Xavier Navarro [5,7]

[1] Neuroengineering Lab, Department of Health Sciences and Technology, Institute for Robotics and Intelligent Systems, ETH Zürich, 8092 Zürich, Switzerland

[2] NEARLab - Neuroengineering and Medical Robotics Laboratory DEIB Department of Electronics, Information and Bioengineering Politecnico di Milano 20133, Milano, Italy

[3] IIT Central Research Labs Genova, Istituto Italiano Tecnologia, 16163 Genova, Italy

[4] The BioRobotics Institute, Scuola Superiore Sant'Anna, I-56127, Pisa, Italy.

[5] Institute of Neurosciences and Department of Cell Biology, Physiology and Immunology, Universitat Autònoma de Barcelona, and CIBERNED, 08193 Bellaterra, Spain.

[6] Translational Neural Engineering Laboratory, Center for Neuroprosthetics and Institute of Bioengineering, Ecole Polytechnique Federale de Lausanne, Lausanne CH-1015, Switzerland.

[7] Institut Guttmann de Neurorehabilitació, Badalona, Spain.

Correspondence to: X Navarro (xavier.navarro@uab.cat) or S Micera (silvestro.micera@epfl.ch).

Declarations of interest: none

"This is a non-final version of an article published in final form in (Journal of Neuroscience Methods, https://doi.org/10.1016/j.jneumeth.2020.108653 )."

**ABSTRACT**

Neurointerfaces have acquired major relevance as both rehabilitative and therapeutic tools for patients with spinal cord injury, limb amputations and other neural disorders. Bidirectional neural interfaces are a key component for the functional control of neuroprosthetic devices. The two main neuroprosthetic applications of interfaces with the peripheral nervous system (PNS) are: the refined control of artificial prostheses with sensory neural feedback, and functional electrical stimulation (FES) systems attempting to generate motor or visceral responses in paralyzed organs. The results obtained in experimental and clinical studies with both, extraneural and intraneural electrodes are very promising in terms of the achieved functionality for the neural stimulation mode. However, the results of neural recordings with peripheral nerve interfaces are more limited. In this paper we review the different existing approaches for PNS signals recording, denoising, processing and classification, enabling their use for bidirectional interfaces. PNS recordings can provide three types of signals: i) population activity signals recorded by using extraneural electrodes placed on the outer surface of the nerve, which carry information about cumulative nerve activity; ii) spike activity signals recorded with intraneural electrodes placed inside the nerve, which carry information about the electrical activity of a set of individual nerve fibers; and iii) hybrid signals, which contain both spiking and cumulative signals. Finally, we also point out some of the main limitations, which are hampering clinical translation of neural decoding, and indicate possible solutions for improvement.

Key words: peripheral nerve, neural interfaces, signal processing, neuroprosthesis, neural decoding.

## 1. Introduction

Neuroprostheses are artificial systems capable of partially restoring or replacing body functions lost after injuries. They currently represent a therapeutic option for spinal cord injured patients, for subjects with a limb amputation or neural disorders. Bidirectional neural interfaces constitute a key component for the control of neuroprosthetic and robotic devices. Neural interfaces can be applied at the brain level (e.g. brain-machine interfaces, brain-computer interfaces) or at the peripheral nerves with the aim to resolve a variety of disabilities or to deliver neuromodulatory therapies.

The use of electrodes applied to the surface or invasively within muscles or in the peripheral nerves for research and for diagnostic purposes has a long history (Kazamel and Warren, 2017). The most common techniques used in clinical neurophysiology comprehend nerve conduction studies, sensory and motor evoked potentials in which the nervous system is stimulated and compound action potentials are recorded most commonly with surface electrodes placed on the skin over the nerve or muscle of interest. In electromyography (EMG) the spontaneous or voluntarily elicited muscle activity is recorded often with intramuscular needle electrodes. A more sophisticated technique is microneurography, in which a thin tungsten needle electrode is inserted within the peripheral nerve for recording action potentials conducted by nerve fibers in the vicinity of the needle tip. Given its technical complexity and time-consuming features, microneurography has limited applications for research purposes in the study of sensory and autonomic functions (Gandevia and Hales, 1997; Vallbo, 2018).

Two of the most relevant applications of interfaces with the somatic peripheral nervous system (PNS) for neuroprostheses with biomedical use are: the bidirectional control of artificial limb-prostheses (with additional neural feedback) and functional electrical stimulation (FES) systems, developed to artificially bridge central motor control and directly stimulate the intact peripheral nerves or muscles of spinal cord injured patients, attempting to generate motor or visceral responses that mimic normal physiological actions. Presently, neurorehabilitation systems commonly suffer the lack of sufficient control sources and absence of feedback sensory information. In order to overcome the aforementioned problems, research in this field is focusing on the investigation of different types of neural electrodes and their related ability of acquiring electroneurographic signals (Navarro et al., 2005). This is of crucial importance in order to improve neural interfaces and design more useful neuroprosthetic systems. In fact, after some pioneering promising results (Micera et al., 2010a, 2011; Rossini et al., 2010), the latest advancements in neural recordings with peripheral nerve interfaces are relatively limited. Recently, some useful results have been reported when using microelectrode arrays placed in the nerves of human amputees (Davis et al., 2016; Wendelken et al., 2017). However, when the amputees attempted to control the prosthetic device, they needed to use

implantable electromyographic (iEMG) signals in combination with the neural ones, in order to achieve a satisfactory motor control. Recently, Clark et al. (2014) demonstrated that offline signal processing can isolate neural activity from EMG, but it has not been incorporated yet for online decoding and prosthetic control.

In contrast, successful demonstrations have been obtained in recent years on the clinical translation of neural stimulation using neural interfaces in amputee patients (Oddo et al., 2016; Ortiz-Catalan et al., 2014; Petrini et al., 2019b; Raspopovic et al., 2014; Tan et al., 2014; Valle et al., 2018) in providing touch and quasi-proprioceptive sensory feedback information. The results obtained with both extraneural and intraneural electrodes are very promising, in terms of the achieved functionality (Oddo et al., 2016; Raspopovic et al., 2014) and stability (Petrini et al., 2019b; Tan et al., 2014).

In the present review, we focus on neural signal analysis in the field of somatic neuroprostheses. We depict the different existing approaches for PNS signals recording, processing, and classification. The main limitations of these methods, which are hampering clinical translation of neural decoding, are discussed and possible solutions for overcoming them indicated.

## 2. Peripheral nerve fibers

The PNS is constituted by groups of neurons whose cell bodies are located in the brainstem and the spinal cord (motor neurons) or in nearby sensory and autonomic ganglia and their axons, which extend along the peripheral nerves to reach target organs. Cranial nerves emerge from the brainstem and provide innervation to cranial organs, while the vagus nerve (X cranial nerve) descends to innervate most visceral organs in the thorax and abdomen. The spinal roots exit from the spinal cord, from cervical to coccygeal levels and form the somatic peripheral nerves that connect muscles, joints and skin with the CNS (Gardner and Bunge, 2005).

In all the peripheral nerves the axons are grouped in fascicles surrounded by supportive connective layers. The epineurium is the outermost layer, continuous with the connective cover of surrounding tissues. It is a loose connective tissue and carries the blood vessels supplying the nerve. The perineurium, that surrounds each fascicle within the nerve, is composed of several layers of flat perineurial cells and an outer layer of dense collagen fibers. The perineurium is the main contributor to the tensile strength of the nerve and maintains a high endoneurial pressure. The endoneurium has fibroblasts, collagen fibers and extracellular matrix, occupying the space between nerve fibers in each fascicle, plus capillary vessels. The endoneurial collagen fibers form the endoneurial tubules,

in which axons run accompanied by Schwann cells which either myelinate or just surround the axons (Peters et al., 1991; Berthold et al., 2005).

Peripheral nerves are anatomically organized in fascicles that along the course of the nerve divide in branches that innervate distinct targets (muscle, skin, vessels, viscera). The fascicular architecture changes throughout the length of the nerve, with increasing number of fascicles of smaller size in more distal segments of the nerve, particularly in the long nerves of the limbs. Several studies in animal species, including monkeys, based on retrograde tracing (Badia et al., 2010; Brushart, 1991; Velde et al., 2004) provided data supporting a systematic fascicular topography in the peripheral nerve, at least in somatic nerves in the limbs. In human nerves, using anatomical dissection, immunohistochemical labeling and computer reconstruction methods, it has been reported that fascicular organization occurs in short segments close to the joints and remains relatively unaltered over centimeter lengths of the nerve (Delgado-Martínez et al., 2016; Watchmaker et al., 1991). Studies using microneurography also suggested a defined somatotopy in human nerve fascicles, and even an intrafascicular segregation by modality of sensory fibers in a given nerve fascicle (Hallin, 1990). Such a topographical defined architecture facilitates selective interfacing of different fascicles within a common nerve with a neural multielectrode device (Badia et al., 2011).

There are several types of nerve fibers within the peripheral nerve, following the historical classification proposed by Erlanger and Gasser (1930). A first division is between unmyelinated or myelinated axons, depending on whether the accompanying Schwann cells only embrace them or develop a multi-lamellae, insulating myelin sheath around them. Unmyelinated C fibers are of small diameter, between 0.5 and 2.0 μm, and impulses propagate along their membrane in a continuous mode, at slow velocity (0.5-1.5 m/s). In myelinated fibers, the myelin cover is arranged as contiguous sheaths of about 1 mm length, with a narrow space of about 1 μm between sheaths, known as node of Ranvier, where ion channels are concentrated. Conduction of impulses in myelinated fibers follows a saltatory course, from node to node, allowing much faster conduction velocity (between 5 and 100 m/s depending on the diameter and myelin thickness). Myelinated nerve fibers are classified in Aα, Aβ, Aγ, Aδ and B types according to size and related conduction velocity.

When using extracellular techniques, the large myelinated fibers have lower resistance to be excited by electrical stimulation, due to the high density of voltage-dependent ion channels at the nodes of Ranvier, than thin myelinated fibers with shorter internodal distances, whereas unmyelinated fibers have a much higher threshold. On the other hand, the extracellular electrical field generated by different types of nerve fibers also differs, being directly related to the axonal caliber (Schoonhoven and Stegeman, 1991; Yoo et al., 2013). This determines that in common nerve conduction tests

using surface electrodes on the skin, only the compound action potentials of myelinated Aα/Aβ nerve fibers are detectable, whereas for recording activity of C fibers more invasive techniques, such as microneurography, are needed (Serra et al., 2010).

Functionally, peripheral nerve fibers are separated in sensory, motor and autonomic fibers, depending on the respective neuron and target connections (Gardner and Bunge, 2005). Most somatic peripheral nerves are mixed, containing motor, sensory and sympathetic axons. Afferent sensory fibers transmit a variety of inputs from mechanical, thermal or noxious stimuli; they can be unmyelinated or myelinated, and terminate at the periphery either as free endings or in specialized receptors in the skin, muscles and deep tissues. Efferent motor axons are myelinated and come from either alpha or gamma motoneurons in the anterior horn of the spinal cord, traveling to establish neuromuscular synapses with skeletal muscle fibers. Efferent autonomic nerve fibers in the somatic peripheral nerves are postganglionic sympathetic fibers, unmyelinated, and go to innervate smooth muscle and glands.

The nervous system controls movement by regulating the contraction of skeletal muscles by increasing the number of motor units activated and their firing frequency. Motor units recruitment follows a strict size order, with slow fatigue-resistant motor units activated first and large fast fatigue motor units activated only at high levels of force (Henneman et al., 1965). Regarding sensory information, different populations of sensory neurons are able to transduce one specific sensory modality depending upon the axonal receptors. Thus, distinct subpopulations of axons are dedicated to convey tactile, proprioceptive, thermal or noxious sensory information from the periphery (Horch et al., 1977). They have also a size-related activation threshold; mechanoreceptive Aα and Aβ fibers are excited with low intensity stimulus, whereas nociceptive Aδ and C fibers have high threshold in physiological conditions (Vallbo, 1981). Signals are transmitted by the corresponding axons in bursts of action potentials, with intensity of the signal mainly coded by the impulse frequency and the number of afferent axons activated. The autonomic nervous system plays an import role in the physiological control of all the visceral systems in the body. Sympathetic and parasympathetic branches trigger opposing actions in most body functions regulation, most often acting on different cells in the organ (Karemaker, 2017). For example, in pacemaker heart cells stimulation sympathetic activation increases whereas parasympathetic stimulation decreases the depolarization rate generating opposite chronotropic effects. In somatic nerves, there are only sympathetic postganlionic fibers supplying the visceral structures in the skin and muscles, i.e. blood vessels, sweat glands and piloerector muscles.

## 3. Nerve electrodes: extra and intraneural

In the case of an interface for the control of a neuroprosthesis in amputees, recording of efferent signals in motor fibers can be used for the activation of the mechanical prosthesis, whereas stimulation of afferent fibers within the residual nerve may provide sensory feedback from tactile and force sensors in the prosthesis. For patients suffering from resistant epilepsy, vagus nerve stimulation has been already used as clinically useful anticonvulsant therapy. Moreover, further experimentations indicate potential clinical applications of autonomic nerve stimulation as antidepressant, mood and cardiac function regulator (George et al. 2002). In motor FES applications, typically stimulation is delivered to motor nerve fibers, over the nerve or at its entrance in the target muscle, to activate the paralyzed muscles, whereas recording the activity of sensory fibers may contribute to close-loop control of the system. Regardless the application, it is of paramount importance that the electrodes interface the selected nerve fiber population as selectively as possible (Grill et al., 2009). Two key factors should be considered for selective interfacing: anatomical selectivity of the targeted population of nerve fibers, that relates to the specific anatomical territory innervated by a given fascicle, and functional selectivity of distinct classes of nerve fibers, that relates with the type of function conveyed by the targeted axons (Micera et al., 2008; 2010a).

Different types of electrode designs have been developed to interface the PNS for different biomedical applications (Navarro et al., 2005; Schultz and Kuiken, 2011; Patil and Thakor, 2016). Nerve electrodes can be classified into three main types depending on invasiveness: extraneural, intraneural and regenerative. These implantable devices have different designs, and thus different procedures for implantation. More invasive electrodes reduce the distance between the active site and the axons, avoiding electrical field spreading, thus decreasing the current intensity needed for stimulation and improving the signal-to-noise ratio for neural recording. With increasing invasiveness of the implanted electrode, higher selectivity may be reached and the recorded signals may have higher amplitude (Badia et al., 2011; 2016). However, extraneural electrodes are often preferable since they are less traumatic for the neural tissue than intraneural ones.

Among the extraneural electrodes, cuff electrodes have been used for many years in FES systems to activate motor axons and induce a muscular response of paralyzed or non-responding muscles. Implants in the radial or ulnar nerves of amputees have been able to provide sensory-like perceptions in different studies (Ortiz-Catalan et al., 2014; Tan et al., 2014). In FES applications using electrical stimulation of efferent nerve fibers, nerve signals recorded from afferent sensory fibers with cuff electrodes have been used for providing sensory cutaneous information in drop foot and hand grasp neuroprostheses (Inmann et al., 2001; Morten and Thomas, 1999), and also on the pelvic nerve and sacral roots to record the neural information from bladder afferents in micturition control devices (Kurstjens et al., 2005). Stimulation selectivity between large fascicles may be achieved by using multipolar cuff electrodes (Navarro et al., 2001; Tarler and Mortimer, 2004).

However, since they are placed around the nerve, cuff electrodes can only record mixed activity of the most superficial nerve fascicles. The Flat Interface Nerve Electrode (FINE) is a design variation that applies a small pressure for flattening the nerve and displacing the axons from the center to the surface, closer to the active sites (Tyler and Durand, 2002). The FINE has been implanted around the femoral nerve trunk in humans to evoke motor responses (Schiefer et al., 2010) and on the median nerve to provide sensory perceptions for feedback (Tan et al., 2014).

Among the intraneural types, the Multielectrode arrays (MEAs) are composed of a rigid base holding tens of needles with electrodes at the tip; they are inserted transversally into the nervous system, thus providing a multi-site recording and stimulation interface. A modified version, named Utah Slanted Electrode Array (USEA), was designed to increase usability with the PNS and proved to allow for selective stimulation of motor fibers and selective recording of single unit responses (Branner et al., 2004; Davis et al., 2016).

Longitudinal Intra-Fascicular Electrodes (LIFEs), initially made of thin insulated conducting wires, were longitudinally inserted into a nerve fascicle and used for microstimulation and for neural recording (Yoshida and Stein, 1999) with lower risk for nerve damage. Horch and colleagues implanted metal LIFEs in the arm nerves of several amputee subjects, as an interface with a neuroprosthetic arm, showing that the recorded signals improved control over its movements and whereas afferent stimulation incorporated useful sensory feedback (Dhillon et al., 2005).

By exploiting the potential of microtechnologies, new designs of thin film, flexible electrodes based on a polyimide substrate have been developed. Such thin-film LIFEs allowed multi-unit peripheral nerve recordings and microstimulation using several sites in one implanted device (Navarro et al., 2007). LIFEs implanted in nerves of human amputees also provided evidence of their effective use for controlling advanced hand prostheses and for delivering sensory feedback (Rossini et al., 2010; Tombini et al., 2012).

Through slight modifications in the design, thin-film polyimide-based microelectrodes have been implanted transversally in the nerve in order to interface several fascicles in the nerve with a single device. The Transverse Intrafascicular Multichannel Electrode (TIME) proved to allow for higher selectivity in microstimulation than the single LIFE and multipolar cuffs (Badia et al., 2011). TIMEs implanted in residual nerves of the arm stump of amputees showed excellent results as a multisite interface for delivering fine sensory feedback, thus improving voluntary motor control of the prosthesis (Oddo et al., 2016; Petrini et al., 2019b; Raspopovic et al., 2014).

### 3.1. Electrode failures

For a successful performance over time in chronic implants for neuroprosthetic applications, the interface has to ensure good biocompatibility, robustness and stability. However, the experience in chronic implantations in humans indicates that there is frequently a reduction in the number of functioning electrode active sites, an increase in the stimulation threshold, and a decrease of the signal-to-noise ratio (SNR) along time (Rossini et al., 2010; Raspopovic et al., 2014; Tan et al., 2014; Warwick et al., 2003), particularly limiting the use of intraneural electrodes. Such failures can be due to electromechanical damage to the metal active sites, fatigue and breaks of the wires and connections, changes in conductivity, induced nerve damage and degeneration, and to the foreign body response against the electrode implant. Significant improvements in materials, designs and fabrication procedures of implantable electrodes have been realized during the last two decades, overpassing the traditional, wafer-based integrated electronics (Patil and Thakor, 2016). To further improve the usability of the neural electrodes, considerable efforts are being devoted in the engineering field for increasing robustness and flexibility at the same time of miniaturizing the electrodes (Boehler et al., 2017; Won et al., 2018; Leber et al., 2019), improving the electrical connectors (Koch et al., 2019), and in the biological field to increase biocompatibility of the substrates and to modulate the foreign body reaction (Lotti et al., 2017; De la Oliva et al., 2019).

### 3.2. Electrode configuration

Electrode parameters such as impedance, selectivity, signal-to-noise ratio SNR and biocompatibility are strongly related to its geometry. In fact, electrode performance may be affected in the miniaturization process of its components. Electrode impedance, for example, is a function of parallel impedances generated from the lead wires, parasitic capacitances and the impedance on the recording site interface. Therefore, electrode impedance gets higher as result of the reduced active sites area; SNR decreases and sensitivity to the electrode to external noise is increased (Yoshida et al., 2017). A wide range of electrode sizes has been used for extracellular recordings in the CNS, the sizes ranging from 10 to 125 μm in diameter. A common assumption is that large electrodes (> 50 μm in diameter) are adequate for recording compound field potentials from a wide neuronal ensemble, while small electrodes (< 20 μm) are more suitable for recording extracellular action potentials generated by few nearby neurons (Rossant et al., 2016). Using arrays containing platinum electrodes of different sizes, it was found that noise and signal attenuation depend more on the electrode impedance than on electrode size; by reducing the impedance of small electrodes by surface modifications, the SNR of axonal action potentials was increased (Viswam et al., 2019). For this reason current micro-electrodes design presents macroporous structures in order to maximize surface for signal acquisition.

The electrode size also affects the selectivity of recording (and stimulating) from a very small axonal population. The smaller the recording site surfaces is, the smaller is the fiber population size that can be targeted. Nevertheless, reduction of the active sites of conventional metal electrodes is lower bounded by the electrode impedance and thermal noise that affect the bandwidth of the electrical recordings (Scholvin et al. 2016). Technological advances have allowed the design of electrodes with multiple recording sites; thus, with a single device it is possible to maximize the sampled volume while reducing the electrode size and the tissue damage due to the implantation. The development of an input/output interface with high channels density for simultaneous multiple recordings requires consideration about multiplexed, external instruments and inter-channel electrical crosstalk. In particular, signal referencing is a crucial step in multi-channel systems in order to minimize the contribution to the acquired signals from other biological interactions. Typically, the signal acquired from a single electrode placed in a region where the neural activity is minimal, is used as reference. This channel is connected as input to a differential amplifier across all channels in order to erase the correlated noise (Kipke, 2017). Finally, the amplifier is connected to an external ground reference that depending on the type of electronics is situated on the implantable electronics enclosure or externally driven to a ground terminal.

Regarding interelectrode distance, it is known from nerve conduction studies that the amplitude of compound nerve action potentials recorded from external electrodes gradually increase with the distance between the active and the reference recording electrodes with the optimum in 3-4 cm (Lee et al., 1993). In experimental studies in small laboratory animals such a distance is limited by anatomical constrain, but still an amplitude-distance relationship exists in the few mm range (Li et al 2014). The amplitude of the action potential is influenced by, among other factors, the inter-electrode distance and the conduction velocity of the fibers. When using extraneural cuff-type electrodes, increasing the inter-electrode separation increases the amplitude of the action potential until the separation approaches the wavelength of the action potential (Stein et al., 1975; Yoshida et al., 2009). Increasing interelectrode spacing for bipolar LIFEs has also been shown to increase the signal amplitude (Yoshida & Stein, 1999). For intraneural multi-electrodes, often a reference electrode in contact with the nerve at a few mm distance is used to improve the SNR (Badia et al., 2016).

An effective method to reject large extraneural noise sources (mainly EMG) when using cuff electrodes is the tripolar electrode configuration: a central electrode is connected to one input of the differential amplifier and two equidistant surrounding electrodes are shorted together and connected to the other input (Stein et al., 1975). Several conditions must be met for this configuration to be effective in the cancellation of extraneural noise (Rahal et al., 2000a): 1) similar impedance of the

two electrodes; 2) the middle electrode must be equidistant between the two ends; 3) similar impedance of the amplifier inputs; 4) the end electrodes should be positioned a few mm away from the cuff ends; 5) the cuff must be well-sealed. Several improvements have been explored to further enhance noise cancellation abilities, such as the adaptive tripolar configuration (Struijk and Thomsen, 1995), the true tripolar configuration (Pflaum et al., 1997), the true tripolar configuration with adaptive balancing (Plachta et al., 2014), the revised quasi-tripolar configuration (Chu et al., 2012; Lee et al., 2016a), and the screened tripole (Rahal et al., 2000b). In general, splitting all contacts into small recording areas to increase the number of electrode sites has negative effects on noise rejection. However, if this is applied only to the central contact creating a mixed tripole configuration, a significant improvement was observed (Ortiz-Catalan et al., 2013).

For intraneural electrodes, such as LIFE and TIME, the different active sites are small round metal electrodes (40-80 μm in diameter) and are placed along the polymer shaft, with inter-electrode spacing of ~230 μm (Lago et al., 2007; Boretius et al., 2010). Though limited to monopolar electrode configurations by having all contacts at longitudinal position, good selectivity in stimulation and recording was demonstrated in acute experiments in rats (Badia et al., 2016, 2011) and pigs (Kundu et al., 2014). Usually, the recorded data contain simultaneous monopolar signals from different active sites of the intraneural electrode. Various papers considered a unipolar configuration as referencing strategy for the signals (see Brychta et al., 2007; Diedrich et al., 2003) while others analyzed signals in bipolar configuration (Kamavuako et al., 2010; Citi et al., 2008; Citi and Micera, 2013). The best monopolar or differential recording pair for a given stimulus was chosen using an automated procedure based on SNR measures (Citi et al., 2008; Citi and Micera, 2013). The highest SNR was often found from the bipolar configuration. In addition to referencing, various signal processing techniques have been employed to separate the noise from the signal thus enhancing the SNR (see Section 4.2). To address the problem of interfering EMG signals, some studies have placed Faraday cages around the nerves, either in the form of a carbon fiber mesh or an insulator cuff (Djilas et al., 2007; Mortimer et al., 1995).

## 4. Electroneurography (ENG) signals: characteristics and processing.

Three types of signals can be recorded from peripheral nerves during functional activity, i.e. spontaneous or evoked by natural stimuli (Figure 1): i) population activity signals recorded by using extraneural interfaces placed on the outer surface of the nerve (e.g. FINE or cuff), which carry information about cumulative nerve activity rather than neuron-specific signaling; ii) spike activity signals recorded with intraneural electrodes placed inside the nerve, either longitudinally or transversally (e.g. LIFE or MEA), which carry information about the electrical activity of a set of

individual nerve fibers (axons); iii) hybrid signals, which contain both spiking and cumulative signals (e.g. as obtained with TIME or microneurographic needles).

### 4.1. Population activity signals detection and processing

Detecting sensory events can drastically improve both control of neuroprostheses and therapeutic strategies. In fact system capability would make possible that the controller algorithms automatically select the best strategy for different detected stimuli. Moreover, the possibility of classifying such information allows the integration, in the case of limb neuroprostheses, of motor reflexes-like behaviors triggered by sensory feedback (Inmann et al., 2001). Durand and colleagues (Wodlinger and Durand, 2011, 2009) have developed very complex beamforming algorithms in an effort to develop the tools to extract the signals of interest from the mixed ones in the volume conductor of the nerve. These algorithms, however, have not been implemented in relevant clinical scenario. Finally, being able to detect only the intention related to the movement, from the mixed peripheral nerve, would potentially enable the voluntary control of the prosthetic device by amputees. Therefore, a lot of work has been performed in recording signals, and implementing algorithms for their processing, trying to develop a tool for the future human translation.

Real-time event detection in neural-related signals, independently from their anatomical and functional nature, goes through standardized blocks: pre-processing, feature extraction and classification (Ahsan et al., 2009; Hong et al., 2018; Wolpaw et al., 2002). Example of how this typical signal processing workflow has been applied in ENG signals in order to detect specific events has been presented in (Raspopovic et al., 2010). Figure 2 shows its schematic representation.

#### 4.1.1. Pre-processing

The pre-processing main objective is the preparation of the signal for the following processing step. Depending on the type of interested events and the type of application, this first block of operations aim to extract from the raw ENS only relevant data to the analysis avoiding contamination due to artifacts and noise. Pre-processing is usually a two-step procedure: the definition of the signals buffering and filter parameters. These are required for windowed analysis in real-time applications and the optimization of the SNR in order to augment the performance of the processing (Fig 2b.).

Real-time applications for ENS analysis based on the running observation window (ROW) requires choosing the optimal values of two main parameters: the window length and the percentage of overlap between two adjacent windows. Overlapping between windows is an important factor in order to avoid mishandling data on buffer boundaries (Hong et al., 2018). These particular parameters are related to the assumption of quasi-stationarity (or local stationarity) of the signals in

a short period of time (Karlsson et al., 2000; Merletti et al., 1992). Therefore, the choice of these parameters mainly depends on the nature of the signal and its particular spectral components (Florian and Pfurtscheller, 1995). Particular deviations may be introduced depending of the type of processing that is planned (Lebedev and Nicolelis, 2006). In fact, several studies have used this kind of approach, both in EMG (Englehart and Hudgins, 2003; Oskoei and Hu, 2008) and EEG signals (Galán et al., 2008; Leeb et al., 2011).

According to the literature, there are no suggested values for ENG windowed analysis parameters; therefore, they have to be chosen experimentally. While window overlap is mostly a function of the processing computing time, a range of different values should be tested for the window lengths. Once identified the values that maximize the output performances, overlap can be adjusted with the same principle without breaking the real-time constraints. Raspopovic et al. (2010) were able to draw certain conclusions about the choice of this parameter values during ENG signal processing: the information contained in features is not stable enough (too biased) for short windows (e.g. 25-50 ms) and a decline in performance was observed for excessively long windows (e.g. 300 ms). The best performance was in the 100 ms window in most cases.

Raw ENG signals recorded with extraneural interfaces have a frequency range typically between 1 kHz and 10 kHz, with maximal spectral power below 3 kHz (Haugland et al., 1994). Lower frequencies carry neural additional information, but due to surrounding muscle activity, which accounts harmonics up to 800 Hz, a cut off has to be applied in order to avoid signal contamination (Nikolić et al., 1994; Zecca et al., 2002). Additional high frequency contributions due to electrode thermal and amplifier noise need to be filtered out (Upshaw and Sinkjaer, 1998). Usually ENG signals are analogically filtered between 1 and 3 KHz before amplification. After signal conversion, different types of digital filters can be used in order to denoise the acquired ENG. In the hypothesis of additive stationary stochastic noise, matched and Wiener filters have been used for maximizing the SNR (Jezernik et al., 2001; Jezernik and Grill, 2001). The performance of such filters is comparable with the common approach of FIR bandpass filtering (Raspopovic et al., 2010); Chebyshev and Butterworth filters are the most used (Jezernik and Grill, 2001; Upshaw and Sinkjaer, 1998). Nonetheless, in order to choose correct values for cutoff frequencies, spectral analysis has to be performed, as explained previously. After band-pass filtering operations have isolated the principal neural signal energy band, the signal can be rectified and smoothed or, in alternative, subspace decomposition algorithms (Upshaw and Sinkjaer, 1998) can be applied to further reduce noise. ENG signals typically carry information from different populations of nerve fibers, each transmitting electrical pulses with different conduction velocity and contributing to specific bands of the frequency spectrum. Then, a narrower band-pass filtering or the application of

optimal filters can further improve the SNR and the identification of specific signal sources (Hong et al., 2018; Jezernik and Grill, 2001).

### 4.1.2. Feature extraction

Due to the relative high dimensionality of the measured data, features extraction is a necessary step in order to reduce the computational burden during data processing (Fig.2c). A feature is the most alternative accurate description of the input variables through a certain attribute, which maximizes the amount of significant characteristics of signal suppressing redundant or undesired information (Guyon et al., 2008). Establishing the function projection of the recorded data toward the feature space generates a subspace with dimension $M < N$, where N is the cardinality of the original one. Behavior decodification from population of ENG signals, similarly to other neural related biosignals, has been addressed exploring different extraction techniques and domains. Time-based features are among the most commonly used: Mean Absolute Value (MAV), Root Mean Square (RMS), Variance (VAR) and Wave Length (WL) are just a few examples of the possible space transformations (Brunton et al., 2017b; Nazmi et al., 2016).

Another type of feature broadly used is the power in discrete frequency bands, that can be extracted as Power Spectral Density (PSD) coefficients in the ROW (Leeb et al., 2013; Nag et al., 2014). Feature composition may rely additionally on wavelet denoising, discrete Fourier transformation, autoregressive and spectral coefficients or autocorrelation-based features (Phinyomark et al., 2012). Several of these types of features extracted from ENG have been presented in (Raspopovic et al., 2010).

In case of classification related applications, performances are strongly influenced from the input used during the training phase, therefore it is necessary to estimate the relevance of the extracted features better discriminating the classes. Performance optimization is probably the most accurate approach in identifying the most significant features through classification testing; moreover, such analysis has to consider possible combinations or subset of inputs, making the process time and computationally consuming (Raspopovic et al., 2010). Neuro-Fuzzy Networks and Genetic Algorithms, or a combination of the two, can be used in order to automate the procedure (Cavallaro et al., 2003). These particular classes of algorithms, soft-computing, allow to generalize the optimization problem through model-free structure allowing to handle the complexity of the neural features.

Multivariate analysis of variance instead aims in assessing the statistical significance of variables differences in the space generated by the totality of the features set. Canonical Variate Analysis (CVA) in particular establishes a sorting method based on the variable's discrimination level (Galán et al., 2008). Regarding direct application of feature selection on ENG signals, Raspopovic et al.

(2010) found that "power-based" features and their combinations performed significantly better with respect to others. This trend was found for every stimulus and their combinations.

### 4.1.3. Classification

Detection of sensory events is essential in case of neuroprosthesis where their discrimination permits the control of predetermined types of actions. Due to the complexity of the human neuro-sensory system, transfer function between the recorded ENG and the desired output behavior is usually unknown. Under these particular conditions machine-learning algorithm can learn from the signals and produce data-driven predictions and decisions, building a consistent mathematical model. Classifiers generally belong to two different families: supervised and unsupervised.

In the supervisor class, data are labeled with the belonging class and the algorithm defines the best separation rule between the set of possible labels. The difference among these classifiers is the shape of the decision boundaries. In ENG pattern classification, supervised machine learning algorithms have been explored through Linear Discriminant analysis (LDA) (Silveira et al., 2018), Super Vector Machine (SVM) (Badia et al., 2016; Micera et al., 2011, 2010b, 2008; Raspopovic et al., 2010) or Artificial Neural Networks (Mirfakhraei and Horch, 1997; Raspopovic et al., 2010; Rossini et al., 2010).

Unsupervised classifiers instead are based on clustering algorithm. Distance among unlabeled input samples in the feature space is typically used in order to group together the data in different classes maximizing within-class similarities. Once the clusters are formed, the separation rule is defined. Among them K-means, fuzzy-C means and density-based clustering are the most used. Broad comments about classifiers applied in neural signals can be found in previous reports (Lotte et al., 2007; Scheme and Englehart, 2011; Zecca et al., 2002).

Machine learning classification problems are divided in two steps: training and testing. Acquired data is therefore consequently separated in two different sets which will be used for the two different stages: both the datasets should carry the same testing conditions in order to avoid model overfitting. Training phase is the process in which the chosen classifier learns from the extracted features and calibrate the discrimination between classes based on its type of rules (Fig 2.d). Validation of the classifier on the testing set consists in the assessment of the ability of the algorithm in predicting the right outcome on novel data (Fig 2.e). Training set and testing sets go through the same pre-processing and feature extraction procedures. Different signal processing on the recorded signals may generate feature values drifts compromising the accuracy of the model predictions.

There is no suggested classifier from the literature for ENG applications. Performance of classifiers strongly depends on the type of pre-processing and feature extraction algorithms that have been implemented. In fact, researchers explore different type of classifiers in order to understand which maximizes the validation performance. This particular iterative step is necessary in order to understand which classification decision boundary fits better the new ENG space derived from previous processing. Such procedure can be eventually avoided through Deep-Learning Classification approaches, but the authors have found no evidence of such application.

Depending on the final application, on the number of classes to be discriminated and on the task to be controlled, the output of the classifier can be going through a final decision-making block (Fig 2.f). This block is particularly important in case of continuous control, which has to integrate the discrete classifier output to a continuous function.

## 4.2. Spiking signals processing

### 4.2.1. Denoising Spiking signals

Raw ENG signals recorded with intraneural interfaces contain information about the spiking activity of neurons encapsulated inside the nerve fascicles. Spikes can be detected and classified by analyzing the high-frequency range of the recorded signals (> 1 kHz). However, an upper cutoff frequency of the filter is chosen to diminish the noisy appearance of spike shapes. Moreover, as for extraneural interfaces, a lower cut off has to be applied to avoid signal contamination. Although there is not a standard band-pass frequency range for the filters, the typical order of magnitude is ~$10^2$ Hz for the lower limit and ~$10^4$ Hz for the upper limit (Diedrich et al., 2003; Dhillon et al., 2004; Micera et al., 2010; Rossini et al., 2010; Noce et al., 2018a).

It has been shown that among the most commonly used techniques, the use of wavelet based denoising can significantly improve the later stages of intraneural ENG signal processing, i.e. spike detection and sorting (Brychta et al., 2007; Citi et al., 2008; Citi and Micera, 2013; Diedrich et al., 2003). Wavelet denoising is widely used in biomedical signals processing with the aim to remove noise from biological signals (Citi et al., 2008; Micera et al., 2010a; Musick et al., 2015; Pani et al., 2016; Rossini et al., 2010; Tombini et al., 2012). The main idea is to decompose the signal at various scales in which a thresholding procedure on the obtained coefficients is able to identify and remove the noise from the signal when transforming back in the original time domain.

Various types of wavelet denoising schemes can be adopted. A standard wavelet-based denoising procedure is implemented via the discrete wavelet transform (DWT), which consists of iterative convolution of high frequency $H(f)$ and low frequency $G(f)$ filters. Additionally, downsampling

and upsampling are performed to obtain a non-redundant representation and signal reconstruction, respectively. However, due to the lack of time translational invariance, it has been shown that DWT decomposition schemes underperform spike detection (Brychta et al., 2007) and classification (Citi et al., 2008; Citi and Micera, 2013). For these reasons other versions of wavelet transformations, such as stationary wavelet transform (SWT) or continuous wavelet transform, have been adopted. The main differences of the SWT with respect to DWT is the absence of downsampling/upsampling and the use of level dependent filters (see for graphical examples Citi and Micera, 2013). The choice of the filter used in the decomposition is related to the adopted mother wavelet. Signal and scaled versions of the mother wavelet are matched and for this reason it is reasonable to choose a wavelet function that resemble the shape of action potentials. Since the action potential form is determined by various factors (e.g. recording electrodes, region of peripheral nervous system) there are no specific rules for the choice of the mother wavelet. Usually, an expert is looking at the recordings and spikes are isolated by visual inspection, thus allowing selecting the mother wavelet that best match the spike waveform (for example in (Citi et al., 2008; Diedrich et al., 2003) a Symmlet 7 wavelet is considered). Optimization algorithms have also been explored (Kamavuako et al., 2010), in which a wavelet is selected based on SNR maximization criterion on the processed output signal.

After the decomposition, a thresholding procedure is applied on the obtained coefficients setting to zero the ones that are thought to reflect noise and maintaining the ones which should reflect the action potentials contribution. Several standard thresholding methods have been considered in the literature depending on the type of assumptions made on the signal. In the case of not uniformly white noise, a level-dependent threshold selection that compute the standard deviation on each level is more suitable to the global standard deviation(Brychta et al., 2007; Citi et al., 2008; Citi and Micera, 2013; Diedrich et al., 2003; Kamavuako et al., 2010). Thus, for each level, a threshold can be selected by implementing a universal threshold or a minimal threshold (Donoho and Johnstone, 1994). The latter provides a more conservative denoising that could be more appropriate when dealing with action potentials at the border of the noise level (a typical situation of peripheral neural recordings). Finally, the signal reconstruction can be done by selecting the level of the decomposition containing relevant information on the neural activity (Brychta et al., 2007; Citi et al., 2008; Citi and Micera, 2013). Inclusion of small or excessively large scales could hinder the performance of wavelet template matching due to decrease of correlation between the signal and the mother wavelet on those scales (Kim and Kim, 2003).

### 4.2.2. Spike detection and sorting

When using intraneural interfaces with high selectivity, it is possible to extract spikes from the signal and assign them to different classes of nerve fibers that relate with the type of function performed by the targeted axons. The high selectivity of intra-neural electrodes enables the development of approaches based on spike detection and sorting techniques borrowed from cortical array signal processing (Diedrich et al., 2003; Brychta et al., 2007; Citi et al., 2008; Citi and Micera, 2013; Noce et al., 2018a; Petrini et al., 2019a). Because different types of nerve fibers can yield different spike shapes, the shape of a spike can be helpful in determining which type of activity is associated with the recorded signal. Spikes in recorded data are normally detected by some algorithm (spike detection algorithm), and may be further sorted based on the spike waveform (by a spike sorting algorithm) according to their shapes, duration, amplitudes and other features.

**a. Spike detection**

The quality of extracellular recording of action potentials by means of microelectrodes inserted in the nerve strongly depends on coupling quality and distance between the firing neuron and the electrode. The amplitude of recorded spikes decreases as a function of neuron distance from the electrode. In some recordings, the amplitude of spikes is comparable to the amplitude of thermal and biological noise (low SNR) turning spike detection, i.e. the identification of spike occurrences, into a non-trivial task. Current spike detection algorithms fall within the four main strategies presented below, although recent work has explored different methodologies, developed in particular for noisy neuronal data, such as fractal dimensions or fuzzy and probability theories (Azami et al., 2015; Azami and Sanei, 2014).

*Amplitude threshold methods*. The spike detection process is performed by using an amplitude threshold to discriminate between spikes and noise. However, how to select the best threshold value is one of the major challenges. If the threshold value is too small, noise fluctuations will lead to false positive events, if it is too large, low-amplitude spikes will be missed, leading to what is called the detection trade-off. A reasonable threshold would be a multiple, typically between 3 and 5 (Kamboh and Mason, 2013; Noce et al., 2018a; Quiroga et al., 2004; Takekawa et al., 2010), of the standard deviation of the noise, $\sigma_N$. To estimate $\sigma_N$, a value based on the standard deviation of the filtered signal, $\sigma_X$, can be used, i.e. threshold = $k \cdot \sigma_X$, where $k$ is a scalar multiplier. However, this approach can lead to high error rates because the signal is a mixture of the noise component, $N$, and the spike component, $S$. Clearly, using the variance of the mixture as an estimate of the variance of the noise will lead to a larger threshold, particularly in the case of high firing rate and large amplitude spikes. If the noise component is assumed to be normally distributed, however, it can be shown that $\sigma_N = \frac{median(|N|)}{0.6745}$ and, as the spike component does not affect much the median absolute

deviation, i.e. $median(|N|) \approx median(|X|)$, the best estimate of $\sigma_N$ would be $\widehat{\sigma_N} = \frac{median(|X|)}{0.6745}$ (Quiroga et al., 2007).

*Energy approach.* In this approach, the instantaneous power of the signal is compared against a threshold derived from the estimated mean and standard deviation of the noise power. The passage from the pre-processed signal to the instantaneous power aims at reducing the effects of the background noise whilst enhancing the spike component of the signal. The instantaneous power is calculated using a running window (online) or a convolution kernel (offline) (Quiroga et al., 2004; Rutishauser et al., 2006; Noce et al., 2018b). Alternatively, the non-linear energy operator (NEO) can be calculated from the pre-processed signal (Lieb et al., 2017). Its performance depends on a threshold that is usually calculated by an approximation formula (Franke et al., 2010), although recently an empirical method for the calculation of an optimal NEO threshold was presented (Malik et al., 2016). While these methods usually offer some improvement over amplitude threshold methods, they perform rather poorly in a low SNR environment (Nenadic and Burdick, 2005).

*Template matching detection*. Another widespread method to detect spikes is based on template matching, i.e. a comparison between putative action potentials and templates representing a typical spike (Franke et al., 2015). First, a waveform that represents a typical spike shape (template) is selected. Then, the method locates possible events in the signal based on similarity measures, e.g. cross-correlation (Friedman, 1968; Kim and McNames, 2007) and Euclidean distance (Sato et al., 2007) of the event and the template. Old template matching methods started with the experimenter manually identifying high-quality spikes, but recently automatic selection algorithms have been successfully introduced (Citi et al., 2008; Liu et al., 2012). Template matching algorithms often detect spike events better than simple threshold algorithms, but their performance depends on a priori knowledge of the spike shape to create the template. Moreover, the automatic selection of a template in a noisy neuronal data can perform poorly in a low SNR environment (Azami and Sanei, 2014; Kim and McNames, 2007).

*Wavelet-based detection*. Action potentials can be directly detected from the detail and approximation coefficients obtained from the application of the Wavelet denoising algorithm (see *Denoising* section). This approach has been demonstrated to outperform the amplitude and the power threshold methods in low SNR environments. The idea is that spike waveforms are not just samples whose average amplitude (or power) exceeds some baseline level, but they also have a characteristic shape and duration. Wavelet-based methods take advantage of this additional information that is ignored by amplitude or power thresholding methods. These algorithms are based on general assumptions on the neural noise, i.e. that it is stationary and Gaussian distributed, and typically consists of three major steps: i) perform multiscale decomposition of the signal using

an appropriate wavelet basis; ii) perform testing at different scales to assess the presence of spikes; iii) estimate the individual spike times.

The method, initially proposed by Nakatani et al. (2001), uses the biorthogonal function *cubic cardinal B-spline* (Chui and Wang, 1992) as wavelet basis for multiscale decomposition of the signal. Later, Nenadic and Burdick (2005) proposed a more robust algorithm for low SNR conditions, which has been used also for PNS recordings (Salmanpour et al., 2010; Micera et al., 2011). They made specific choices for the wavelet basis, by using a biorthogonal 1.3 or 1.5 mother wavelet, and for the restriction of the set of scales and translation, which is based on the sampling rate of the signal, its duration, and expected minimum and maximum spike durations. They performed Bayesian sequential hypothesis testing at different scales to assess the presence of spikes and used parameter estimation methods to accurately extract the occurrence times of individual spikes from the signal. With minimal a priori knowledge about the signal, the algorithm can even be used in an unsupervised manner.

**b. Spike sorting**

The goal of spike sorting is to assign detected spike waveforms to different putative neural units. The spike sorting process typically consists of two phases: feature extraction and cluster separation (Rey et al., 2015). In the first phase, each detected spike, which is an array of $N$ samples, i.e. a point in a $N$-dimensional space, is transformed to a point in a $M$-dimensional space, typically with $M < N$, which is called the feature space. Features are new variables captured from the $N$-dimensional array representing the spike (e.g. spike amplitude, spike duration, etc.; see Lewicki (1998) for a review). One of the major challenges is how to select the best features allowing for optimal separation of different spike clusters. In general, the more discriminative the features, the better the ability to distinguish different spike waveforms. Features such as peak amplitude or width were shown to be poorly discriminative (Quiroga et al., 2004) and currently the main options used by spike sorting algorithms are two: principal components (Abeles and Goldstein, 1977; Lewicki, 1998; Shoham et al., 2003) and wavelets (Hulata et al., 2002; Quiroga et al., 2004; Takekawa et al., 2010; Djilas et al., 2010).

Principal components (PCs) are a set of linearly uncorrelated variables extracted from a set of observations of possibly correlated variables (the detected spike waveforms) by means of an orthogonal transformation. PCs are ordered on the basis of how much variability of the initial data they can account for. In principal component analysis (PCA) each initial spike waveform is transformed into a point in a new $N$-dimensional space, where the coordinates represent the associated scores of the linear combination of the PCs representing the original signal. Using the first PCs, typically 2 or 3, most of the energy in the data (more than 80%) is captured and clusters

representing putative different neurons are visible in a 2-D or 3-D feature space as clouds of points to be separated.

PCA identifies directions of maximum variance in the original dataset, which are not necessarily the ones of maximum separation between spike shapes. Variance within the cloud of points representing a particular spike shape can hide the boundaries between the different clusters, leading to poor cluster separation performance. Variance within waveform groups can be reduced, hence improving the overall performance of PCA. A further step, i.e. spike alignment, is typically needed in which waveforms are aligned at their minimum or maximum peak values. Nevertheless, it has been shown that better performance in cluster separation can be achieved by using wavelet decomposition rather than PCA (Quiroga et al., 2004). The coefficients representing the spike waveform decomposition are the coordinates of a point into a new $N$-dimensional space. By using wavelets, very localized shape differences in the spikes of individual units can be discerned, because i) wavelet coefficients are localized in time, and ii) the information about the shape of the spike will be distributed in several wavelet coefficients, increasing the directions of maximum separation between clusters, compared to PCs. Unlike PCA, however, cluster separation cannot be performed manually when using wavelets, as cluster cannot be visualized in a 3-D (or lower dimensional) space.

In the second step of spike sorting algorithms, spikes with similar features are grouped into clusters that correspond to putative different neural units. Manual clustering can be performed, in which the experimenter defines the boundaries for the different clusters. Although still widely used, this strategy has several drawbacks (Gray et al., 1995; Harris et al., 2000; Pedreira et al., 2012): i) analysis can be performed on two- or maximum three-dimensional projections of the feature space which can be suboptimal, thus leading to poor separation performance; ii) it is very time consuming and is typically a trial-and-error procedure; iii) it is prone to human biases and errors. A number of semi-automatic clustering methods have been also proposed, in which the experimenter specifies the probable number of clusters, such as K-means (Djilas et al., 2010; Jin and Han, 2010; Lewicki, 1998; Webb, 2002) and Expectation-Maximization (Harris et al., 2000; Pouzat et al., 2002). These methods are based on the assumption that clusters are spherically distributed in the feature space, i.e. that spike variability is determined only by additive and Gaussian stationary background noise. In several experimental conditions, however, clusters are non-spherically shaped leading to inherent difficulty to capture the structure of data with a mixture of Gaussians. Alternatives are using a different mixture of distribution, such as t-distributions (Shoham et al., 2003), or nonparametric algorithms such as Valley-Seeking clustering (Koontz and Fukunaga, 1972), hierarchical clustering (Fee et al., 1996) or super-paramagnetic clustering (Quiroga et al., 2004). Fully automatic versions

of these algorithms also exist, which perform an iterative scanning procedure to select the best number of well-separated clusters, as discussed, for example, in Wood and Black (2008), Bestel et al. (2012), Nguyen et al. (2015), and Chung et al. (2017).

Alternative algorithms for spike sorting avoiding the feature extraction and clustering stages also exist. Template matching, for example, is a particularly appealing option when online sorting is necessary, given its simplicity and low computational cost. Once the templates are computed with an offline sorter, or manually identified by the experimenter by choosing high-quality spike shapes, they can be used for template matching, in order to classify each new detected spike online (Citi et al., 2008; Rossini et al., 2010). In line, adaptive template matching (Diedrich et al., 2003; Kim and McNames, 2007; Rutishauser et al., 2006) re-computes templates adaptively as the spikes are detected, thus avoiding over-reliance on a priori knowledge of spike shapes.

### 4.3. Hybrid signals processing

Sometimes, the characteristics of recorded signals are between the cumulative ones (section 4.1.) and the selective, spiking signals (section 4.2.). Such hybrid type of signals have been recorded from TIME electrodes implanted in rats (Badia et al., 2016), enabling the development of the processing and classification scheme, which is exploiting the steps from both population-like and spike-like signals.

Recently, a very interesting approach has been proposed (Petrini et al., 2019a) in order to record human neural signals, during activities of motor control, which could potentially help to develop more robust recording schemes and processing algorithms. By using microneurographic and concurrent EMG recordings (for the purpose of excluding any muscular signal correlated), the authors successfully recorded a variety of neural signals, related to the execution of different force levels, velocities of movement execution, and different types of grasping. This approach is replicable in laboratories worldwide, and could provide valuable datasets for further work in the field of signal processing.

An interesting “hybrid venue” for the prosthesis motor control has been recently exploited (Davis et al., 2016; Wendelken et al., 2017), in which the authors explored the combination of available iEMG and ENG signals in order to decode several degrees of freedom of prosthesis control. It will be very exciting to discern if this approach would enable also a stable control over time, and not only during laboratory controlled trials.

## 5. Limitations of ENG decoding and future challenges

An important question, which arises from the literature, and especially from the recent clinical efforts with human amputees is: ”Why neural stimulation appears to be so robust and functional, whereas recording from the PNS, which has been the goal of extensive animal and human experimentation, is still unstable and unpredictable?” This phenomenon was already observed by Johnson et al. (2005) in brain neural implants, who proposed that the answer to this question stands in the physics of the interaction between the peripheral nerve and the recording/stimulating device. Through computational efforts (Raspopovic et al., 2017) and in vivo studies (de la Oliva et al., 2018a, 2018b), we learned that over time fibrotic tissue grows around the electrode; this biological response can be overcome by increasing the injected charge of stimulation (de la Oliva et al., 2019; Raspopovic et al., 2017). Therefore, only the changes in the current necessary for the device functioning over time are observed, while the functionality is intact. Of interest, passing voltage pulses through a neural microelectrode in vivo implanted in the brain was shown to cause a reduction in electrode impedance and of the SNR, thus improving signal recordings; a procedure termed “rejuvenation” (Otto et al., 2006). However, a similar study in the peripheral nerve has not been reported. On the other side, the model of recording (Gold et al., 2006) teaches us that beyond a certain distance (in the brain, depending on the electrode type, less than 140 μm (Henze et al., 2000)) it is impossible to record the neuronal cell activity anymore. In this case, of course, it is impossible to “increase the neuron signal amplitude” and the recorded units are lost.

Also, in comparison with brain recordings, the peripheral nerve is very hostile, being near structures that are moving all the time (as muscles, tendons etc.) and provoking interferences and noise in the tiny signals to record, and also changing the relative distance between the source of the signal (neurons) and recorder (implantable electrode). The use of hybrid models (Raspopovic et al., 2011), together with extensive animal validation (Raspopovic et al., 2012), would enable to test novel geometries of the devices and their optimal placement (Delgado-Martínez et al., 2016).

An important alternative to the use of the direct neural interfacing, is to exploit “natural amplifiers” of the neural activity, which are designed by the nature: the muscles. Indeed, recently very promising results have been obtained in the recording from the upper limb amputees residual muscle (Pasquina et al., 2015) and their use in the online prosthetic control. In the lower limb, similar technology gave promising outcomes for the real-time ankle control by a transtibial amputee (Kristjansson et al., 2017). Certainly, this approach is mostly viable in the case of distal amputations, where residual muscles are present, while in the more proximal cases, the interest and need for the development of robust recording devices is still important. This triggers the need of developing novel devices and signal processing algorithms, which would enable their clinical application.

**Acknowledgments**

This work was partially supported by the European Research Council Starting Grant ERC StG FeelAgain (contract number 759998), European Union FPT-ICT projects NEBIAS (contract number FP7-611687), FLAG-ERA JTC 2017 project GRAFIN, grant PCI2018-093029 from Ministerio de Ciencia, Innovación y Universidades of Spain, TERCEL (RD12/0019/0011) and CIBERNED (CB06/05/1105) funds from Instituto de Salud Carlos III of Spain, and by Fundación Ramón Areces (CIVP18A3897), the Bertarelli Foundation and the Swiss National Competence Center for Research (NCCR) Robotics.

**References**

Abeles, M., Goldstein, M.H., 1977. Multispike train analysis. Proc. IEEE 65, 762–773. doi:10.1109/PROC.1977.10559.

Ahsan, R., Ibrahimy, M.I., Khalifa, O., 2009. EMG signal classification for human computer interaction : a review. Eur. J. Sci. Research 33, 480–501.

Azami, H., Escudero, J., Darzi, A., Sanei, S., 2015. Extracellular spike detection from multiple electrode array using novel intelligent filter and ensemble fuzzy decision making. J. Neurosci. Methods 239, 129–138. doi:10.1016/j.jneumeth.2014.10.006.

Azami, H., Sanei, S., 2014. Spike detection approaches for noisy neuronal data: Assessment and comparison. Neurocomputing 133, 491–506. doi:10.1016/j.neucom.2013.12.006.

Badia, J., Boretius, T., Andreu, D., Azevedo-Coste, C., Stieglitz, T., Navarro, X., 2011. Comparative analysis of transverse intrafascicular multichannel, longitudinal intrafascicular and multipolar cuff electrodes for the selective stimulation of nerve fascicles. J. Neural Eng. 8, 036023. doi:10.1088/1741-2560/8/3/036023.

Badia, J., Pascual-Font, A., Vivó, M., Udina, E., Navarro, X., 2010. Topographical distribution of motor fascicles in the sciatic-tibial nerve of the rat. Muscle Nerve 42, 192–201. doi:10.1002/mus.21652.

Badia, J., Raspopovic, S., Carpaneto, J., Micera, S., Navarro, X., 2016. Spatial and functional selectivity of peripheral nerve signal recording with the transversal intrafascicular multichannel electrode (TIME). IEEE Trans. Neural Syst. Rehabil. Eng. 24, 20–27. doi:10.1109/TNSRE.2015.2440768.

Berthold, C.H., Fraher, J., King, R.H.M. Microscopic anatomy of the PNS. In: Dyck, P., Thomas, P.K., Peripheral Neuropathy, 4th ed, Saunders, 2005.

Bestel, R., Daus, A.W., Thielemann, C., 2012. A novel automated spike sorting algorithm with adaptable feature extraction. J. Neurosci. Methods 211, 168–178. doi:10.1016/j.jneumeth.2012.08.015.

Boehler, C., Oberueber, F., Schlabach, S., Stieglitz, T., Asplund, M., 2017. Long-term stable adhesion for conducting polymers in biomedical applications: IrOx and nanostructured platinum solve the chronic challenge. ACS Appl. Mater. Interfaces 9, 189-197. doi: 10.1021/acsami.6b13468.

Boretius, T., Badia, J., Pascual-Font, A., Schuettler, M., Navarro, X., Yoshida, K., Stieglitz, T., 2010. A transverse intrafascicular multichannel electrode (TIME) to interface with the

peripheral nerve. Biosens. Bioelectron. 26, 62–69. https://doi.org/10.1016/j.bios.2010.05.010.

Branner, A., Stein, R.B., Fernandez, E., Aoyagi, Y., Normann, R.A., 2004. Long-term stimulation and recording with a penetrating microelectrode array in cat sciatic nerve. IEEE Trans. Biomed. Eng. 51, 146–157. doi:10.1109/TBME.2003.820321.

Brunton, E., Blau, C., Silveira, C., Nazarpour, K., 2017a. Identification of sensory information in mixed nerves using multi-channel cuff electrodes for closed loop neural prostheses, in: International IEEE/EMBS Conference on Neural Engineering, NER. pp. 391–394. doi:10.1109/NER.2017.8008372.

Brunton, E., Blau, C.W., Nazarpour, K., 2017b. Separability of neural responses to standardised mechanical stimulation of limbs. Sci. Rep. 7, 11138. doi:10.1038/s41598-017-11349-z

Brushart, T.M.E., 1991. Central course of digital axons within the median nerve of macaca mulatta. J. Comp. Neurol. 311, 197–209. doi:10.1002/cne.903110203.

Brychta, R.J., Shiavi, R., Robertson, D., Diedrich, A., 2007. Spike detection in human muscle sympathetic nerve activity using the kurtosis of stationary wavelet transform coefficients. J. Neurosci. Methods 160, 359–367. doi:10.1016/j.jneumeth.2006.09.020.

Cavallaro, E., Micera, S., Dario, P., Jensen, W., Sinkjær, T., 2003. On the intersubject generalization ability in extracting kinematic information from afferent nervous signals. IEEE Trans. Biomed. Eng. 50, 1063–1073. doi:10.1109/TBME.2003.816075.

Chu, J.-U., Song, K.-I., Han, S., Lee, S.H., Kim, J., Kang, J.Y., Hwang, D., Suh, J.-K.F., Choi, K., Youn, I., 2012. Improvement of signalto-interference ratio and signal-to-noise ratio in nerve cuff electrode systems. Physiol. Meas. 33, 943–967. doi.org/10.1088/0967-3334/33/6/943.

Chui, C.K., Wang, J. zhong, 1992. A general framework of compactly supported splines and wavelets. J. Approx. Theory 71, 263–304. doi:10.1016/0021-9045(92)90120-D

Chung, J.E., Magland, J.F., Barnett, A.H., Tolosa, V.M., Tooker, A.C., Lee, K.Y., Shah, K.G., Felix, S.H., Frank, L.M., Greengard, L.F., 2017. A fully automated approach to spike sorting. Neuron 95, 1381-1394.e6. doi:10.1016/j.neuron.2017.08.030.

Citi, L., Carpaneto, J., Yoshida, K., Hoffmann, K.P., Koch, K.P., Dario, P., Micera, S., 2008. On the use of wavelet denoising and spike sorting techniques to process electroneurographic signals recorded using intraneural electrodes. J. Neurosci. Methods 172, 294–302. doi:10.1016/j.jneumeth.2008.04.025.

Citi, L., Micera, S., 2013. Wavelet denoising and conditioning of neural recordings, in: Introduction to neural engineering for motor rehabilitation. pp. 173–182. doi:10.1002/9781118628522.ch9.

Clark, G.A., et al. 2014. Using multiple high-count electrode arrays in human median and ulnar nerves to restore sensorimotor function after previous transradial amputation of the hand. 2014 36th Annual International Conference of the IEEE Engineering in Medicine and Biology Society.

Davis, T.S., Wark, H.A.C.C., Hutchinson, D.T., Warren, D.J., O'Neill, K., Scheinblum, T., Clark, G.A., Normann, R.A., Greger, B., O'Neill, K., Scheinblum, T., Clark, G.A., Normann, R.A., Greger, B., 2016. Restoring motor control and sensory feedback in people with upper extremity amputations using arrays of 96 microelectrodes implanted in the median and ulnar nerves. J. Neural Eng. 13, 036001. doi:10.1088/1741-2560/13/3/036001.

De la Oliva, N., Del Valle, J., Delgado-Martinez, I., Mueller, M., Stieglitz, T., Navarro, X., 2019. Long-term functionality of transversal intraneural electrodes is improved by dexamethasone treatment. IEEE Trans. Neural Syst. Rehabil. Eng. 27, 457–464. doi:10.1109/tnsre.2019.2897256.

De la Oliva, N., Mueller, M., Stieglitz, T., Navarro, X., Del Valle, J., 2018a. On the use of Parylene C polymer as substrate for peripheral nerve electrodes. Sci. Rep. 8, 5965. doi:10.1038/s41598-018-24502-z.

De la Oliva, N., Navarro, X., del Valle, J., 2018b. Time course study of long-term biocompatibility and foreign body reaction to intraneural polyimide-based implants. J. Biomed. Mater. Res. - Part A 106, 746–757. doi:10.1002/jbm.a.36274.

Delgado-Martínez, I., Badia, J., Pascual-Font, A., Rodríguez-Baeza, A., Navarro, X., 2016. Fascicular topography of the human median nerve for neuroprosthetic surgery. Front. Neurosci. 10. doi:10.3389/fnins.2016.00286.

Dhillon, G.S., Krüger, T.B., Sandhu, J.S., Horch, K.W., 2005. Effects of short-term training on sensory and motor function in severed nerves of long-term human amputees. J. Neurophysiol. 93, 2625–2633. doi:10.1152/jn.00937.2004.

Diedrich, A., Charoensuk, W., Brychta, R.J., Ertl, A.C., Shiavi, R., 2003. Analysis of raw microneurographic recordings based on wavelet de-noising technique and classification algorithm: Wavelet analysis in microneurography. IEEE Trans. Biomed. Eng. 50, 41–50. doi:10.1109/TBME.2002.807323.

Djilas, M., Yoshida, K., Kurstjens, M., Azevedo-Coste, C., 2007. Improving the signal-to-noise ratio in recordings with thin-film longitudinal intra-fascicular electrodes using shielding cuffs. 2007 3rd International IEEE/EMBS Conference on Neural Engineering. pp. 167–170. doi.org/10.1109/CNE.2007.369638.

Donoho, D.L., Johnstone, J.M., 1994. Ideal spatial adaptation by wavelet shrinkage. Biometrika 81, 425–455. doi:10.1093/biomet/81.3.425.

Englehart, K., Hudgins, B., 2003. A robust, real-time control scheme for multifunction myoelectric control. IEEE Trans. Biomed. Eng. 50, 848–854. doi:10.1109/TBME.2003.813539.

Erlanger, J., Gasser, H.S., 1930. The action potential in fibers of slow conduction in spinal roots and somatic nerves. Am. J. Physiol. 92, 43-82.

Fee, M.S., Mitra, P.P., Kleinfeld, D., 1996. Automatic sorting of multiple unit neuronal signals in the presence of anisotropic and non-Gaussian variability. J. Neurosci. Methods 69, 175–188. doi:10.1016/S0165-0270(96)00050-7

Florian, G., Pfurtscheller, G., 1995. Dynamic spectral analysis of event-related EEG data. Electroencephalogr. Clin. Neurophysiol. 95, 393–396. doi:10.1016/0013-4694(95)00198-8

Franke, F., Natora, M., Boucsein, C., Munk, M.H.J., Obermayer, K., 2010. An online spike detection and spike classification algorithm capable of instantaneous resolution of overlapping spikes. J. Comput. Neurosci. 29, 127–148. doi:10.1007/s10827-009-0163-5

Franke, F., Quian Quiroga, R., Hierlemann, A., Obermayer, K., 2015. Bayes optimal template matching for spike sorting – combining fisher discriminant analysis with optimal filtering. J. Comput. Neurosci. 38, 439–459. doi:10.1007/s10827-015-0547-7

Friedman, D.H., 1968. Detection of signals by template matching. Baltimore: Johns Hopkins Press.

Galán, F., Nuttin, M., Lew, E., Ferrez, P.W., Vanacker, G., Philips, J., Millán, J. del R., 2008. A brain-actuated wheelchair: Asynchronous and non-invasive brain-computer interfaces for continuous control of robots. Clin. Neurophysiol. 119, 2159–2169.

Gandevia, S.C., Hales, J.P. 1997. The methodology and scope of human microneurography. J. Neurosci. Methods 74, 123-36.

Gardner, E., Bunge, R.P., 2005. Gross anatomy of the PNS In: Dyck, P., Thomas, P.K., Peripheral Neuropathy, 4th ed, Saunders.

George, M.S., Nahas, Z., Bohning, D.E., Kozel, F.A., Anderson, B., Chae, J.H., Lomarev, M., Denslow, S., Li, X., Mu, C., 2002. Vagus nerve stimulation therapy: a research update. Neurology 59, S56-S61.

Gold, C., Henze, D.A., Koch, C., Buzsáki, G., 2006. On the origin of the extracellular action potential waveform: a modeling study. J. Neurophysiol. 95, 3113–3128. doi:10.1152/jn.00979.2005

Gray, C.M., Maldonado, P.E., Wilson, M., McNaughton, B., 1995. Tetrodes markedly improve the reliability and yield of multiple single-unit isolation from multi-unit recordings in cat striate cortex. J. Neurosci. Methods 63, 43–54. doi:10.1016/0165-0270(95)00085-2

Grill, W.M., Norman, S.E., Bellamkonda, R.V., 2009. Implanted neural interfaces: biochallenges and engineered solutions. Annu. Rev. Biomed. Eng. 11, 1-24. doi:10.1146/annurev-bioeng-061008-124927.

Guyon, I., Gunn, S., Nikravesh, M., Zadeh, L., 2008. Feature extraction: foundations and applications (Vol. 207). Springer.

Hallin, R.G., 1990. Microneurography in relation to intraneural topography: Somatotopic organisation of median nerve fascicles in humans. J. Neurol. Neurosurg. Psychiatry 53, 736–744. doi:10.1136/jnnp.53.9.736

Harris, K.D., Henze, D.A., Csicsvari, J., Hirase, H., Buzsáki, G., 2000. Accuracy of tetrode spike separation as determined by simultaneous intracellular and extracellular measurements. J. Neurophysiol. 84, 401–14. doi:10.1152/jn.2000.84.1.401

Haugland, M.K., Hoffer, J.A., Sinkjær, T., 1994. Skin contact force information in sensory nerve signals recorded by implanted cuff electrodes. IEEE Trans. Rehabil. Eng. 2, 18–28. doi:10.1109/86.296346

Haugland, M., Sinkjaer, T., 1999. Interfacing the body's own sensing receptors into neural prosthesis devices. Technol. Health Care 7, 393-399.

Henneman, E., Somjen, G., Carpenter, Do., 1965. Functional significance of cell size in spinal motoneurons. J. Neurophysiol. 28, 560-580.

Henze, D.A., Borhegyi, Z., Csicsvari, J., Mamiya, A., Harris, K.D., Buzsáki, G., 2000. Intracellular features predicted by extracellular recordings in the hippocampus in vivo. J. Neurophysiol. 84, 390-400.

Hong, K.S., Aziz, N., Ghafoor, U., 2018. Motor-commands decoding using peripheral nerve signals: A review. J. Neural Eng. 15, 031004. doi:10.1088/1741-2552/aab383

Horch, K.W., Tuckett, R.P., Burgess, P.R., 1977. A key to the classification of cutaneous mechanoreceptors. J. Invest. Dermatol. 69, 75-82.

Hulata, E., Segev, R., Ben-Jacob, E., 2002. A method for spike sorting and detection based on wavelet packets and Shannon’s mutual information. J. Neurosci. Methods 117, 1–12. doi:10.1016/S0165-0270(02)00032-8

Inmann, A., Haugland, M., Haase, J., Biering-Sørensen, F., Sinkjaer, T., 2001. Signals from skin

mechanoreceptors used in control of a hand grasp neuroprosthesis. Neuroreport 12, 2817–2820. doi:10.1097/00001756-200109170-00013

Jezernik, S., Grill, W.M., 2001. Optimal filtering of whole nerve signals. J. Neurosci. Methods 106, 101–110. doi:10.1016/S0165-0270(01)00334-X

Jezernik, S., Grill, W.W., Sinkjaer, T., 2001. Neural network classification of nerve activity recorded in a mixed nerve. Neurol. Res. 23, 429–434. doi:10.1179/016164101101198811

Jin, X., Han, J., 2010. K-Means Clustering, in: Sammut, C., Webb, G.I. (Eds.), Encyclopedia of Machine Learning. Springer US, Boston, MA, pp. 563–564. doi:10.1007/978-0-387-30164-8_425

Johnson, M.D., Otto, K.J., Kipke. D.R., 2005. Repeated voltage biasing improves unit recordings by reducing resistive tissue impedances. IEEE Trans. Neural Syst Rehab Eng 13.2, 160-165.

Kamavuako, E.N., Jensen, W., Yoshida, K., Kurstjens, M., Farina, D., 2010. A criterion for signal-based selection of wavelets for denoising intrafascicular nerve recordings. J. Neurosci. Methods 186, 274–280. doi:10.1016/j.jneumeth.2009.11.022

Kamboh, A.M., Mason, A.J., 2013. Computationally efficient neural feature extraction for spike sorting in implantable high-Density recording systems. IEEE Trans. Neural Syst. Rehabil. Eng. 21, 1–9. doi:10.1109/TNSRE.2012.2211036

Karemaker, J.M., 2017. An introduction into autonomic nervous function. Physiol. Meas. 38, R89-R118. doi: 10.1088/1361-6579/aa6782.

Karlsson, S., Yu, J., Akay, M., 2000. Time-frequency analysis of myoelectric signals during dynamic contractions: A comparative study. IEEE Trans. Biomed. Eng. 47, 228–238. doi:10.1109/10.821766

Kazamel, M., Warren, P.P., 2017. History of electromyography and nerve conduction studies: A tribute to the founding fathers. J. Clin. Neurosci. 43, 54-60. doi: 10.1016/j.jocn.2017.05.018.

Kim, K.H., Kim, S.J., 2003. A wavelet-based method for action potential detection from extracellular neural signal recording with low signal-to-noise ratio. IEEE Trans. Biomed. Eng. 50, 999–1011. doi:10.1109/tbme.2003.814523

Kim, S., McNames, J., 2007. Automatic spike detection based on adaptive template matching for extracellular neural recordings. J. Neurosci. Methods 165, 165–174. doi:10.1016/j.jneumeth.2007.05.033

Kipke, D.R., 2017. CNS recording devices and techniques. In: Horch, K.W., Dhillon G.S. (eds.) Neuroprosthetics: theory and practice. Second Edition. World Scientific. p. 479-480

Koch, J., Schuettler, M., Pasluosta, C., Stieglitz, T., 2019. Electrical connectors for neural implants: design, state of the art and future challenges of an underestimated component. J. Neural. Eng. 16, 061002. doi: 10.1088/1741-2552/ab36df.

Koontz, W.L.G., Fukunaga, K., 1972. A nonparametric valley-seeking technique for cluster analysis. IEEE Trans. Comput. C–21, 171–178. doi:10.1109/tc.1972.5008922

Kristjansson, K., Sigurdardottir, J.S., Sverrisson, A., Sigurthorsson, S.P., Sverrisson, O., Einarsson, A., Lechler, K., Ingvarsson, T., Oddsson, M., 2017. Prosthetic control by lower limb amputees using implantable myoelectric sensors, in: Biosystems and Biorobotics. Springer, Cham, pp. 571–574. doi:10.1007/978-3-319-46669-9_94.

Kundu, A., Harreby, K.R., Yoshida, K., Boretius, T., Stieglitz, T., Jensen, W., 2014. Stimulation selectivity of the "thin-film longitudinal intrafascicular electrode" (tfLIFE) and the "transverse intrafascicular multi-channel electrode" (TIME) in the large nerve animal model. IEEE Trans. Neural Syst. Rehabil. Eng. 22, 400–410. doi.org/10.1109/TNSRE.2013.2267936.

Kurstjens, G.A.M., Borau, A., Rodríguez, A., Rijkhoff, N.J.M., Sinkjær, T., 2005. Intraoperative recording of electroneurographic signals from cuff electrodes on extradural sacral roots in spinal cord injured patients. J. Urol. 174, 1482–1487. doi:10.1097/01.ju.0000173005.70269.9c

Lago, N., Yoshida, K., Koch, K.P., Navarro, X., 2007. Assessment of biocompatibility of chronically implanted polyimide and platinum intrafascicular electrodes. IEEE Trans. Biomed. Eng. 54, 281–290. doi.org/10.1109/TBME.2006.886617

Lebedev, M.A., Nicolelis, M.A.L., 2006. Brain-machine interfaces: past, present and future. Trends Neurosci. 29, 536–546. doi:10.1016/j.tins.2006.07.004

Leber, M., Körner, J., Reiche, C.F., Yin, M., Bhandari, R., Franklin, R., Negi, S., Solzbacher, F., 2019. Advances in penetrating multichannel microelectrodes based on the Utah Array platform. Adv. Exp. Med. Biol. 1101, 1-40. doi: 10.1007/978-981-13-2050-7_1.

Lee, H.J., DeLisa, J.A., Bach, J.R., 1993. Physiologic considerations in the determination of optimum interelectrode distance for the antidromic recording of compound sensory nerve action potentials. Am. J. Phys. Med. Rehabil. 72:99-100.

Lee, Y.J., Kim, H.-J., Do, S.H., Kang, J.Y., Lee, S.H., 2016a. Characterization of nerve-cuff electrode interface for biocompatible and chronic stimulating application. Sens. Actuators B Chem. 237, 924–934. doi.org/10.1016/j.snb.2016.06.169.

Leeb, R., Perdikis, S., Tonin, L., Biasiucci, A., Tavella, M., Creatura, M., Molina, A., Al-Khodairy, A., Carlson, T., Millán, J. d. R., 2013. Transferring brain-computer interfaces beyond the

laboratory: Successful application control for motor-disabled users. Artif. Intell. Med. 59, 121–132. doi:10.1016/j.artmed.2013.08.004

Leeb, R., Sagha, H., Chavarriaga, R., Millán, J.D.R., 2011. A hybrid brain-computer interface based on the fusion of electroencephalographic and electromyographic activities. J. Neural Eng. 8, 025011. doi:10.1088/1741-2560/8/2/025011

Lewicki, M.S., 1998. A review of methods for spike sorting: The detection and classification of neural action potentials. Netw. Comput. Neural Syst. 9. doi:10.1088/0954-898X_9_4_001

Li, Y., Lao, J., Zhao, X., Tian, D., Zhu, Y., Wei, X., 2014. The optimal distance between two electrode tips during recording of compound nerve action potentials in the rat median nerve. Neural. Regen. Res. 9:171–178. doi: 10.4103/1673-5374.125346.

Lieb, F., Stark, H.G., Thielemann, C., 2017. A stationary wavelet transform and a time-frequency based spike detection algorithm for extracellular recorded data. J. Neural Eng. 14, 036013. doi:10.1088/1741-2552/aa654b

Liu, X., Yang, X., Zheng, N., 2012. Automatic extracellular spike detection with piecewise optimal morphological filter. Neurocomputing 79, 132–139. doi:10.1016/j.neucom.2011.10.016

Lotte, F., Congedo, M., Lécuyer, A., Lamarche, F., Arnaldi, B., 2007. A review of classification algorithms for EEG-based brain-computer interfaces. J. Neural Eng. 4, R1–R13. doi:10.1088/1741-2560/4/2/R01

Lotti, F., Ranieri, F., Vadalà, G., Zollo, L., Di Pino, G., 2017. Invasive intraneural interfaces: foreign body reaction issues. Front. Neurosci. 11, 497. doi: 10.3389/fnins.2017.00497.

Malik, M.H., Saeed, M., Kamboh, A.M., 2016. Automatic threshold optimization in nonlinear energy operator based spike detection, in: Proceedings of the Annual International Conference of the IEEE Engineering in Medicine and Biology Society, EMBS. pp. 774–777. doi:10.1109/EMBC.2016.7590816

Merletti, R., Knaflitz, M., DeLuca, C.J., 1992. Electrically evoked myoelectric signals. Crit. Rev. Biomed. Eng. 19, 293–340.

Micera, S., Carpaneto, J., Raspopovic, S., 2010a. Control of hand prosthesis using peripheral information. Biomed. Eng. IEEE Rev. 3, 48–68.

Micera, S., Citi, L., Rigosa, J., Carpaneto, J., Raspopovic, S., Di Pino, G., Rossini, L., Yoshida, K., Denaro, L., Dario, P., Rossini, P.M., 2010b. Decoding information from neural signals recorded using intraneural electrodes: Toward the development of a neurocontrolled hand prosthesis. Proc. IEEE 98, 407–417. doi:10.1109/JPROC.2009.2038726

Micera, S., Navarro, X., Carpaneto, J., Citi, L., Tonet, O., Rossini, P.M., Carrozza, M.C., Hoffmann, K.P., Vivó, M., Yoshida, K., Dario, P., 2008. On the use of longitudinal intrafascicular peripheral interfaces for the control of cybernetic hand prostheses in amputees. IEEE Trans. Neural Syst. Rehabil. Eng. 16, 453–472. doi:10.1109/TNSRE.2008.2006207

Micera, S., Rossini, P.M., Rigosa, J., Citi, L., Carpaneto, J., Raspopovic, S., Tombini, M., Cipriani, C., Assenza, G., Carrozza, M.C., Hoffmann, K.-P.P., Yoshida, K., Navarro, X., Dario, P., 2011. Decoding of grasping information from neural signals recorded using peripheral intrafascicular interfaces. J. Neuroeng. Rehabil. 8, 53. doi:10.1186/1743-0003-8-53

Mirfakhraei, K., Horch, K., 1997. Recognition of temporally changing action potentials in multiunit neural recordings. IEEE Trans. Biomed. Eng. 44, 123–131. doi:10.1109/10.552242

Morten, H., Thomas, S., 1999. Interfacing the body's own sensing receptors into neural prosthesis devices. Technol. Heal. Care 7, 393–9.

Mortimer, T., Agnew, W.F., Horch, K., Citron, P., Creasey, G., Kantor, C., 1995. Perspectives on new electrode technology for stimulating peripheral nerves with implantable motor prostheses. IEEE Trans. Rehabil. Eng. 3, 145–154. doi.org/10.1109/86.392373.

Musick, K.M., Rigosa, J., Narasimhan, S., Wurth, S., Capogrosso, M., Chew, D.J., Fawcett, J.W., Micera, S., Lacour, S.P., 2015. Chronic multichannel neural recordings from soft regenerative microchannel electrodes during gait. Sci. Rep. 5, 14363. doi:10.1038/srep14363.

Nag, S., Ng, K.A., Jagadeesan, R., Sheshadri, S., Delgado-Martinez, I., Bossi, S., Yen, S.C., Thakor, N. V., 2014. Neural prosthesis for motor function restoration in upper limb extremity. IEEE 2014 Biomedical Circuits and Systems Conference, BioCAS 2014 - Proceedings. pp. 388–391. doi:10.1109/BioCAS.2014.6981744.

Nakatani, H., Watanabe, T., Hoshimiya, N., 2001. Detection of nerve action potentials under low signal-to-noise ratio condition. IEEE Trans. Biomed. Eng. 48, 845–849. doi:10.1109/10.936360.

Navarro, X., Krueger, T.B., Lago, N., Micera, S., Stieglitz, T., Dario, P., 2005. A critical review of interfaces with the peripheral nervous system for the control of neuroprostheses and hybrid bionic systems. J. Peripher. Nerv. Syst. 10, 229–58. doi:10.1111/j.1085-9489.2005.10303.x

Navarro, X., Lago, N., Vivó, M., Yoshida, K., Koch, K.P., Poppendieck, W., Micera, S., 2007. Neurobiological evaluation of thin-film longitudinal intrafascicular electrodes as a peripheral nerve interface. 2007 IEEE 10th International Conference on Rehabilitation Robotics, ICORR'07. pp. 643–649. doi:10.1109/ICORR.2007.4428492.

Navarro, X., Valderrama, E., Stieglitz, T., Schüttler, M., 2001. Selective fascicular stimulation of the rat sciatic nerve with multipolar polyimide cuff electrodes. Restor. Neurol. Neurosci. 18, 9–21.

Nazmi, N., Rahman, M.A.A., Yamamoto, S.I., Ahmad, S.A., Zamzuri, H., Mazlan, S.A., 2016. A review of classification techniques of EMG signals during isotonic and isometric contractions. Sensors (Switzerland) 16, 1304. doi:10.3390/s16081304.

Nenadic, Z., Burdick, J.W., 2005. Spike detection using the continuous wavelet transform. IEEE Trans. Biomed. Eng. 52, 74–87. doi:10.1109/TBME.2004.839800.

Nguyen, T., Bhatti, A., Khosravi, A., Haggag, S., Creighton, D., Nahavandi, S., 2015. Automatic spike sorting by unsupervised clustering with diffusion maps and silhouettes. Neurocomputing 153, 199–210. doi:10.1016/j.neucom.2014.11.036.

Nikolić, Z.M., Popović, D.B., Stein, R.B., Kenwell, Z., 1994. Instrumentation for ENG and EMG recordings in FES systems. IEEE Trans. Biomed. Eng. 41, 703–706. doi:10.1109/10.301739.

Noce, E., Ciancio, A.L., Zollo, L., 2018. Spike detection: The first step towards an ENG-based neuroprosheses. J. Neurosci. Methods 308, 294–308. doi:10.1016/j.jneumeth.2018.07.008.

Oddo, C.M., Raspopovic, S., Artoni, F., Mazzoni, A., Spigler, G., Petrini, F., Giambattistelli, F., Vecchio, F., Miraglia, F., Zollo, L., Di Pino, G., Camboni, D., Carrozza, M.C., Guglielmelli, E., Rossini, P.M., Faraguna, U., Micera, S., 2016. Intraneural stimulation elicits discrimination of textural features by artificial fingertip in intact and amputee humans. Elife 5, e09148. doi:10.7554/eLife.09148.

Ortiz-Catalan, M., Håkansson, B., Brånemark, R., Hakansson, B., Branemark, R., 2014. An osseointegrated human-machine gateway for long-term sensory feedback and motor control of artificial limbs. Sci. Transl. Med. 6, 257re6-257re6. doi:10.1126/scitranslmed.3008933.

Ortiz-Catalan, M., Marin-Millan, J., Delbeke J., Hakansson, B., Branemark, R, 2013. Effect on signal-to-noise ratio of splitting the continuous contacts of cuff electrodes into smaller recording areas. J. Neuroeng. Rehab. 10, 22. doi.org/10.1186/1743-0003-10-22.

Oskoei, M.A., Hu, H., 2008. Support vector machine-based classification scheme for myoelectric control applied to upper limb. IEEE Trans. Biomed. Eng. 55, 1956–1965. doi:10.1109/TBME.2008.919734.

Otto, K.J., Johnson, M.D., Kipke, D.R., 2006. Voltage pulses change neural interface properties and improve unit recordings with chronically implanted microelectrodes. IEEE Trans. Biomed. Eng. 53, 333-340.

Pani, D., Barabino, G., Citi, L., Meloni, P., Raspopovic, S., Micera, S., Raffo, L., 2016. Real-time neural signals decoding onto off-the-shelf DSP processors for neuroprosthetic applications. IEEE Trans. Neural Syst. Rehabil. Eng. 24, 993–1002. doi:10.1109/TNSRE.2016.2527696.

Pasquina, P.F., Evangelista, M., Carvalho, A.J., Lockhart, J., Griffin, S., Nanos, G., McKay, P., Hansen, M., Ipsen, D., Vandersea, J., Butkus, J., Miller, M., Murphy, I., Hankin, D., 2015. First-in-man demonstration of a fully implanted myoelectric sensors system to control an advanced electromechanical prosthetic hand. J. Neurosci. Methods 244, 85–93. doi:10.1016/j.jneumeth.2014.07.016.

Patil, A.C., Thakor, N.V., 2016. Implantable neurotechnologies: a review of micro- and nanoelectrodes for neural recording. Med. Biol. Eng. Comput. 54, 23-44. doi: 10.1007/s11517-015-1430-4.

Pedreira, C., Martinez, J., Ison, M.J., Quian Quiroga, R., 2012. How many neurons can we see with current spike sorting algorithms? J. Neurosci. Methods 211, 58–65. doi:10.1016/j.jneumeth.2012.07.010.

Peters, A., Palay, S., Webster, H. deF., 1991. The fine structure of the nervous system: Neurons and their supporting cells, 3rd ed., New York University Press, New York. doi:10.1002/ana.410040660.

Petrini, F., Mazzoni, A., Rigosa, J., Giambattistelli, F., Granata, G., Barra, B., Pampaloni, A., Guglielmelli, E., Zollo, L., Capogrosso, M., Micera, S., Raspopovic, S., 2019a. Microneurography as a tool to develop decoding algorithms for peripheral neuro-controlled hand prostheses. Biomed. Eng. Online 18, 44. doi:10.1186/s12938-019-0659-9.

Petrini, F., Valle, G., Strauss, I., Granata, G., Iorio, R. Di, D'Anna, E., Cvancara, P., Mueller, M., Carpaneto, J., Clemente, F., Controzzi, M., Bisoni, L., Carboni, C., Barbaro, M., Andreu, D., Hiairrassary, A., Divoux, J.L., Cipriani, C., Guiraud, D., Raffo, L., Fernandez, E., Stieglitz, T., Raspopovic, S., Rossini, P.M., Micera, S., 2019b. Six-months assessment of a hand prosthesis with intraneural tactile feedback. Ann Neurol 85, 137–154. doi:10.1002/ana.25384.

Pflaum, C., Riso, R.R., Wiesspeiner, G., 1997. Performance of alternative amplifier configurations for tripolar nerve cuff recorded ENG. Proceedings of 18th Annual International Conference of the IEEE Engineering in Medicine and Biology Society. pp. 375–376. doi.org/10.1109/IEMBS.1996.657000.

Phinyomark, A., Phukpattaranont, P., Limsakul, C., 2012. Feature reduction and selection for EMG signal classification. Expert Syst. Appl. 39, 7420–7431. doi:10.1016/j.eswa.2012.01.102.

Plachta, D.T.T., Gierthmuehlen, M., Cota, O., Espinosa, N., Boeser, F., Herrera, T.C., Stieglitz, T., Zentner, J., 2014. Blood pressure control with selective vagal nerve stimulation and minimal side effects. J. Neural Eng. 11, 036011. doi.org/10.1088/1741- 2560/11/3/036011.

Pouzat, C., Mazor, O., Laurent, G., 2002. Using noise signature to optimize spike-sorting and to assess neuronal classification quality. J. Neurosci. Methods 122, 43–57.

Quiroga, R.Q., Nadasdy, Z., Ben-Shaul, Y., 2004. Unsupervised spike detection and sorting with wavelets and superparamagnetic clustering. Neural Comput. 16, 1661–1687. doi:10.1162/089976604774201631.

Quiroga, R.Q., Reddy, L., Koch, C., Fried, I., 2007. Decoding Visual Inputs From Multiple Neurons in the Human Temporal Lobe. J. Neurophysiol. 98, 1997–2007. doi:10.1152/jn.00125.2007.

Rahal, M., Winter, J., Taylor, J., Donaldson, N., 2000b. An improved configuration for the reduction of EMG in electrode cuff recordings: a theoretical approach. IEEE Trans. Biomed. Eng. 47, 1281–1284. doi.org/10.1109/10.867963.

Rahal, M., Taylor, J., Donaldson, N., 2000a. The effect of nerve cuff geometry on interference reduction: a study by computer modeling. IEEE Trans. Biomed. Eng. 47, 136–138. doi.org/10.1109/10.817629.

Raspopovic, S., Capogrosso, M., Badia, J., Navarro, X., Micera, S., 2012. Experimental validation of a hybrid computational model for selective stimulation using transverse intrafascicular multichannel electrodes. IEEE Trans. Neural Syst. Rehabil. Eng. 20, 395–404. doi:10.1109/TNSRE.2012.2189021.

Raspopovic, S., Capogrosso, M., Micera, S., 2011. A computational model for the stimulation of rat sciatic nerve using a transverse intrafascicular multichannel electrode. IEEE Trans. Neural Syst. Rehabil. Eng. 19, 333–344. doi:10.1109/TNSRE.2011.2151878.

Raspopovic, S., Capogrosso, M., Petrini, F., Bonizzato, M., Rigosa, J., Pino, G. Di, Carpaneto, J., Controzzi, M., Boretius, T., Fernandez, E., Granata, G., Oddo, C.M., Citi, L., Ciancio, A.L., Cipriani, C., Carrozza, M.C., Jensen, W., Guglielmelli, E., Stieglitz, T., Rossini, P.M., Micera, S., 2014. Restoring natural sensory feedback in real-time bidirectional hand prostheses. Sci. Transl. Med. 6, 222ra19. doi:10.1126/scitranslmed.3006820.

Raspopovic, S., Carpaneto, J., Udina, E., Navarro, X., Micera, S., 2010. On the identification of sensory information from mixed nerves by using single-channel cuff electrodes. J. Neuroeng. Rehabil. 7, 17. doi:10.1186/1743-0003-7-17.

Raspopovic, S., Petrini, F., Zelechowski, M., Valle, G., 2017. Framework for the development of neuroprostheses: from basic understanding by sciatic and median nerves models to bionic legs and hands. Proc. IEEE 105, 34–49. doi:10.1109/JPROC.2016.2600560

Rey, H.G., Pedreira, C., Quian Quiroga, R., 2015. Past, present and future of spike sorting techniques. Brain Res. Bull. 119, 106–117. doi:10.1016/j.brainresbull.2015.04.007

Rossant, C., Kadir, S. N., Goodman, D. F. M., Schulman, J., Belluscio, M., Buzsaki, G., et al., 2016. Spike sorting for large, dense electrode arrays. Nat. Neurosci. 19, 634–641. doi: 10.1038/nn.4268.

Rossini, P.M., Micera, S., Benvenuto, A., Carpaneto, J., Cavallo, G., Citi, L., Cipriani, C., Denaro, L., Denaro, V., Di Pino, G., Ferreri, F., Guglielmelli, E., Hoffmann, K.P., Raspopovic, S., Rigosa, J., Rossini, L., Tombini, M., Dario, P., 2010. Double nerve intraneural interface implant on a human amputee for robotic hand control. Clin. Neurophysiol. 121, 777–783. doi:10.1016/j.clinph.2010.01.001

Rutishauser, U., Schuman, E.M., Mamelak, A.N., 2006. Online detection and sorting of extracellularly recorded action potentials in human medial temporal lobe recordings, in vivo. J. Neurosci. Methods 154, 204–224. doi:10.1016/j.jneumeth.2005.12.033

Sato, T., Suzuki, T., Mabuchi, K., 2007. Fast automatic template matching for spike sorting based on Davies-Bouldin validation indices, in: Annual International Conference of the IEEE Engineering in Medicine and Biology - Proceedings. pp. 3200–3203. doi:10.1109/IEMBS.2007.4353010

Scheme, E., Englehart, K., 2011. Electromyogram pattern recognition for control of powered upper-limb prostheses: State of the art and challenges for clinical use. J. Rehabil. Res. Dev. 48, 643. doi:10.1682/jrrd.2010.09.0177

Schiefer, M.A., Polasek, K.H., Triolo, R.J., Pinault, G.C.J., Tyler, D.J., 2010. Selective stimulation of the human femoral nerve with a flat interface nerve electrode. J. Neural Eng. 7, 363–397. doi:10.1088/1741-2560/7/2/026006

Scholvin, J., Kinney, J.P., Bernstein, J.G., Moore-Kochlacs, C., Kopell, N., Fonstad, C.G., Boyden, E.S., 2016. Close-packed silicon microelectrodes for scalable spatially oversampled neural recording. IEEE Trans. Biomed. Eng. 63:120-130. doi: 10.1109/TBME.2015.2406113.

Schoonhoven, R., Stegeman, D.F., 1991. Models and analysis of compound nerve action potentials. Crit. Rev. Biomed. Eng. 19, 47-111.

Schultz, A.E., Kuiken, T.A., 2011. Neural interfaces for control of upper limb prostheses: the state

of the art and future possibilities. PMR 3, 55–67. doi:10.1016/j.pmrj.2010.06.016

Serra, J., Bostock, H., Navarro, X., 2010. Microneurography in rats: a minimally invasive method to record single C-fiber action potentials from peripheral nerves in vivo. Neurosci. Lett. 470, 168-174.

Shoham, S., Fellows, M.R., Normann, R.A., 2003. Robust, automatic spike sorting using mixtures of multivariate t-distributions. J. Neurosci. Methods 127, 111–122. doi:10.1016/S0165-0270(03)00120-1

Silveira, C., Brunton, E., Spendiff, S., Nazarpour, K., 2018. Influence of nerve cuff channel count and implantation site on the separability of afferent ENG. J. Neural Eng. 15, 046004. doi:10.1088/1741-2552/aabca0

Stein, R.B., Charles, D., Davis, L., Jhamandas, J., Mannard, A., Nichols, T.R., 1975. Principles underlying new methods for chronic neural recording. Can. Sci. Neurol. 2, 235–244.

Struijk, J.J., Thomsen, M., 1995. Tripolar nerve cuff recording: stimulus artifact, EMG and the recorded nerve signal. Proceedings of 17th International Conference of the Engineering in Medicine and Biology Society. pp. 1105–1106. https://doi.org/10.1109/IEMBS.1995.579534.

Takekawa, T., Isomura, Y., Fukai, T., 2010. Accurate spike sorting for multi-unit recordings. Eur. J. Neurosci. 31, 263–272. doi:10.1111/j.1460-9568.2009.07068.x

Tan, D.W., Schiefer, M.A., Keith, M.W., Anderson, J.R., Tyler, J., Tyler, D.J., 2014. A neural interface provides long-term stable natural touch perception. Sci. Transl. Med. 6, 257ra138-257ra138. doi:10.1126/scitranslmed.3008669

Tarler, M.D., Mortimer, J.T., 2004. Selective and independent activation of four motor fascicles using a four contact nerve-cuff electrode. IEEE Trans. Neural Syst. Rehabil. Eng. 12, 251–257. doi:10.1109/TNSRE.2004.828415

Tombini, M., Rigosa, J., Zappasodi, F., Porcaro, C., Citi, L., Carpaneto, J., Rossini, P.M., Micera, S., 2012. Combined analysis of cortical (EEG) and nerve stump signals improves robotic hand control. Neurorehabil. Neural Repair 26, 275–281. doi:10.1177/1545968311408919

Tyler, D.J., Durand, D.M., 2002. Functionally selective peripheral nerve stimulation with a flat interface nerve electrode. IEEE Trans. Neural Syst. Rehabil. Eng. 10, 294–303. doi:10.1109/TNSRE.2002.806840

Upshaw, B., Sinkjaer, T., 1998. Digital signal processing algorithms for the detection of afferent nerve activity recorded from cuff electrodes. IEEE Trans. Rehabil. Eng. 6, 172–181. doi:10.1109/86.681183

Vallbo, Å.B., 1981. Sensations evoked from the glabrous skin of the human hand by electrical stimulation of unitary mechanosensitive afferents. Brain Res. 215, 359–363.

Vallbo, Å.B., 2018. Microneurography: how it started and how it works. J. Neurophysiol. 120, 1415-1427. doi: 10.1152/jn.00933.2017.

Valle, G., Mazzoni, A., Iberite, F., D'Anna, E., Strauss, I., Granata, G., Controzzi, M., Clemente, F., Rognini, G., Cipriani, C., Stieglitz, T., Petrini, F.M., Rossini, P.M., Micera, S., D'Anna, E., 2018. Biomimetic intraneural sensory feedback enhances sensation naturalness, tactile sensitivity, and manual dexterity in a bidirectional prosthesis. Neuron 100, 37-45.e7. doi:10.1016/j.neuron.2018.08.033

Velde, K., Ross, M.W., Orsini, J.A., Parente, E.J., Foley, B., Richardson, D.W., Miselis, R.R., 2004. Tracing axons of peripheral nerves in rats: A potential technique to study the equine recurrent laryngeal nerve. J. Investig. Surg. 17, 151–162. doi:10.1080/08941930490446937

Viswam, V., Obien, M.E.J., Franke, F., Frey, U., Hierlemann, A., 2019. Optimal electrode size for multi-scale extracellular-potential recording from neuronal assemblies. Front. Neurosci. 13, 385. doi: 10.3389/fnins.2019.00385.

Watchmaker, G.P., Gumucio, C.A., Crandall, R.E., Vannier, M.A., Weeks, P.M., 1991. Fascicular topography of the median nerve: A computer based study to identify branching patterns. J. Hand Surg. Am. 16, 53–59. doi:10.1016/S0363-5023(10)80013-9

Webb, A., 2002. Statistical pattern recognition. John Wiley & Sons, Ltd.

Wendelken, S., Page, D.M., Davis, T., Wark, H.A.C.C., Kluger, D.T., Duncan, C., Warren, D.J., Hutchinson, D.T., Clark, G.A., 2017. Restoration of motor control and proprioceptive and cutaneous sensation in humans with prior upper-limb amputation via multiple Utah Slanted Electrode Arrays (USEAs) implanted in residual peripheral arm nerves. J. Neuroeng. Rehabil. 14, 121. doi:10.1186/s12984-017-0320-4

Wodlinger, B., Durand, D.M., 2011. Selective recovery of fascicular activity in peripheral nerves. J. Neural Eng. 8, 056005. doi:10.1088/1741-2560/8/5/056005

Wodlinger, B., Durand, D.M., 2009. Localization and recovery of peripheral neural sources with beamforming algorithms. IEEE Trans. Neural Syst. Rehabil. Eng. 17, 461–468. doi:10.1109/TNSRE.2009.2034072

Wolpaw, J.R., Birbaumer, N., McFarland, D.J., Pfurtscheller, G., Vaughan, T.M., 2002. Brain-computer interfaces for communication and control. Clin. Neurophysiol. 113, 767–791. doi:10.1016/S1388-2457(02)00057-3

Won, S.M., Song, E., Zhao, J., Li, J., Rivnay, J., Rogers, J.A., 2018. Recent advances in materials, devices, and systems for neural interfaces. Adv. Mater. 30, e1800534. doi: 10.1002/adma.201800534.

Wood, F., Black, M.J., 2008. A nonparametric Bayesian alternative to spike sorting. J. Neurosci. Methods 173, 1–12. doi:10.1016/j.jneumeth.2008.04.030

Yoo, P.B., Lubock, N.B., Hincapie, J.G., Ruble, S.B., Hamann, J.J., Grill, W.M., 2013. High-resolution measurement of electrically-evoked vagus nerve activity in the anesthetized dog. J Neural Eng. 10, 026003.

Yoshida, K., Bertram, M., Cox, T.G.H., Riso, R.R., 2017. Peripheral nerve recording electrodes and techniques. In: Horch, K.W., Dhillon G.S. (eds.) Neuroprosthetics: theory and practice. Second Edition. World Scientific, 2017.p. 379-387.

Yoshida, K., Kurstjens, G.A., Hennings, K., 2009. Experimental validation of the nerve conduction velocity selective recording technique using a multi-contact cuff electrode. Med. Eng. Phys. 31, 1261-70. doi: 10.1016/j.medengphy.2009.08.005.

Yoshida, K., Stein, R.B., 1999. Characterization of signals and noise rejection with bipolar longitudinal intrafascicular electrodes. IEEE Trans. Biomed. Eng. 46, 226–234. doi:10.1109/10.740885

Zecca, M., Micera, S., Carrozza, M.C., Dario, P., 2002. Control of multifunctional prosthetic hands by processing the electromyographic signal. Crit. Rev. Biomed. Eng. 30, 459–85. doi:10.1615/critrevbiomedeng.v45.i1-6.150

# FIGURES

## FIGURE 1

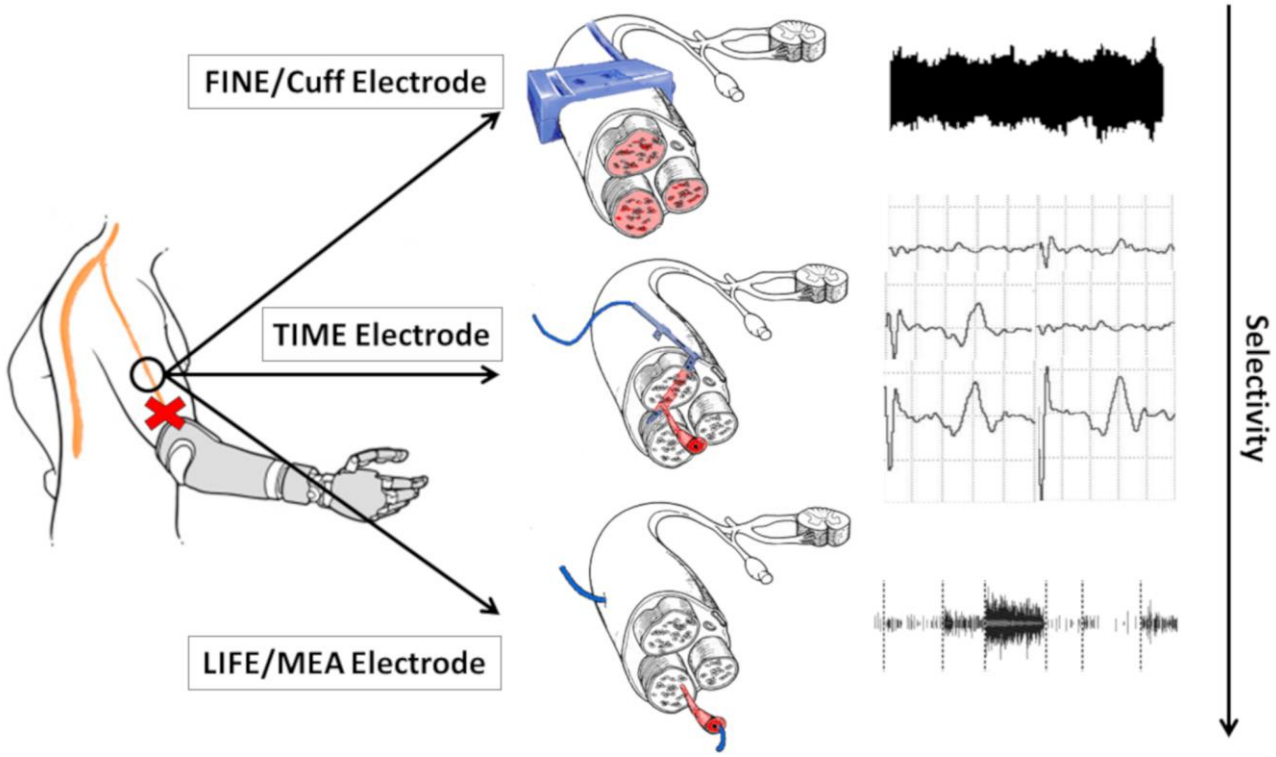


Figure 1. Different types of peripheral nerve interfaces and their respective recording selectivity. On the left, schematic representation of an amputee wearing a prosthesis where communication is interrupted between the device and the nervous system. In the middle, from top to bottom cuff, TIME and LIFE electrodes placement representation (the electrode is marked in blue and the stimulated fiber is red). On the right side, samples of corresponding recorded signals.

**FIGURE 2**

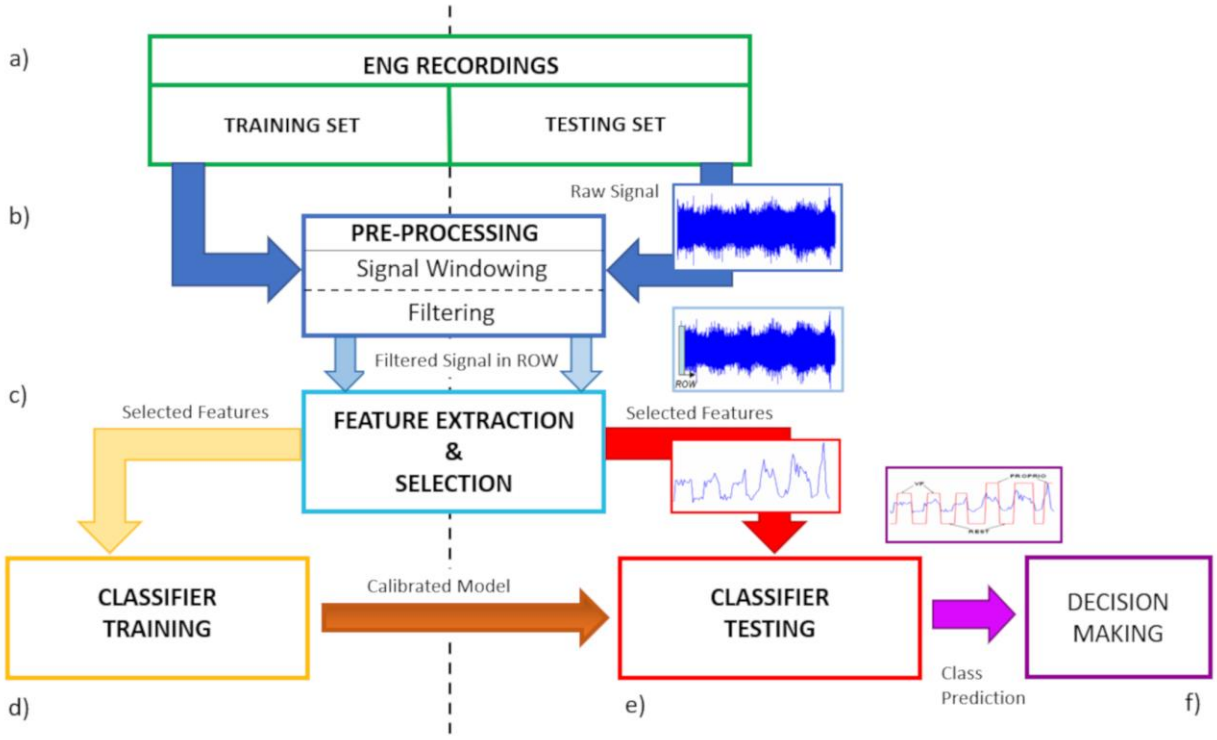


Figure 2. Schematic representation of nerve signals processing for ENG classification; a) Recorded ENG dataset is divided in training and testing set; b) Pre-processing block applies signal segmentation and denoising; c) Feature extraction and selection from the running observation window (ROW); d) Data-driven training of the classification model; e) Validation on the extracted features from the testing set using the calibrated model from the training for class prediction; f) Decision making rule for driving the device based on the classifier outcome.